1067

Proc. 18th Int. Conf. on Low Temperature Physics, Kyoto, 1987
Japanese Journal of Applied Physics, Vol. 26 (1987) Supplement 26-3

EM17

Dynamics of the Phase Transition of Periodic Superconducting Networks

B. JEANNERET, Ch. LEEMANN, and P. MARTINOLI

Institut de Physique, Université de Neuchâtel, CH-2000 Neuchâtel, Switzerland

Proc. 18th Int. Conf. on Low Temperature Physics, Kyoto, 1987
Japanese Journal of Applied Physics, Vol. 26 (1987) Supplement 26-3

Dynamics of the Phase Transition of Periodic Superconducting Networks

B. JEANNERET, Ch. LEEMANN, and P. MARTINOLI

Institut de Physique, Université de Neuchâtel, CH-2000 Neuchâtel, Switzerland

The critical behaviour of superconducting networks, as deduced from a study of the complex ac response of the system as a function of temperature, is found consistent with the vortex unbinding idea of the Kosterlitz-Thouless theory. The ac response of networks exposed to a perpendicular magnetic field shows a complex oscillatory dependence on the reduced flux per unit cell $f = \phi/\phi_0$, with structures at integer and half-integer values of f.

The critical behaviour of superconducting networks [1,2] is expected to be quite similar to that of two-dimensional (2D) arrays of Josephson junctions, where the superconducting-to-normal transition has been shown [2,3] to be driven by the vortex unbinding mechanism predicted by the Kosterlitz-Thouless (KT) theory [4]. In the case of wire networks the nodes can be thought of as regions of strong superconductivity connected by strips which are effectively acting as Josephson weak links with a linear current-phase relationship [2]. Thermal fluctuations in the phase of the superconducting order parameter at the nodal sites generate, in addition to spin-wave excitations, bound vortex-antivortex pairs whose dissociation at a critical temperature T_c triggers the onset of the resistive transition. Fluctuations in the magnitude of the order parameter, on the other hand, are responsible for the mean-field transition of the network, which occurs at a temperature $T_{co} > T_c$. In wire networks with moderate normal-state resistance, T_c is very close to T_{co} [2], i.e. the two transitions essentially merge into a single one. As a consequence, studies of the phase boundary based on purely *resistive* measurements are usually discussed in terms of a linearized mean-field Ginzburg-Landau theory [5,6]. In this letter we report measurements of the *complex dynamic conductance* G of wire networks, an experiment which allows to identify the characteristic features of the KT vortex unbinding transition below the network's mean-field transition.

Granular aluminum films, approximately 400 Å thick, were evaporated onto silicon wafers and patterned using standard photolithography and wet etching. The resulting grid of aluminum wires of width $w \simeq 1.4$ μm forms a square array of $N \times N \simeq 10^6$ nodes with lattice parameter $a = 8$ μm and strip resistance $R_s = 95$ Ω. Measurements of G were performed with a two-coil mutual-inductance technique described elsewere [3]. In the weak screening limit, the signal voltage δV detected by the receive coil is proportional to G and can be expressed by [3] :

$$\delta V = C\omega^2 I_D G \quad , \qquad (1)$$

where ω and I_D are, respectively, the angular frequency and the amplitude of the driving current and C a constant depending on the sample-coil geometry. Neglecting the contribution of normal currents to the ac response, the network impedance $Z = G^{-1}$ can be written as $Z(\omega,T) = i\omega L_K(T)\,\varepsilon(\omega,T)$, where $L_K(T) = \hbar/2ei_c(T)$ is the bare kinetic inductance of the network and $\varepsilon(\omega,T)$ the complex

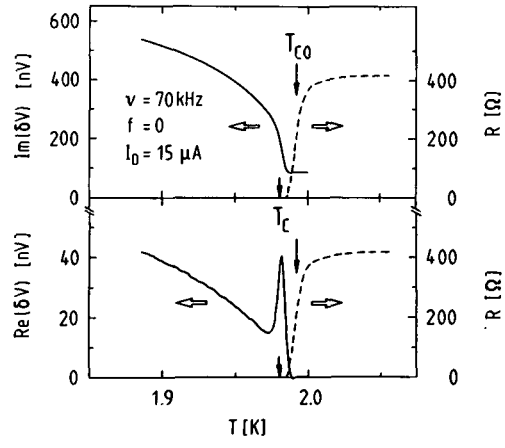

Fig. 1. Temperature dependence of the complex ac response and of the dc resistance in the critical region of an Aℓ-network.

dielectric constant which describes the screening properties of the vortex medium in the critical region [3]. For $w \gg \xi(T)$, the limit of interest here, the critical current $i_c(T)$ of a weak link is related to the bare 2D superfluid density $n_s^*(T)$ by $i_c(T) = (w/L)\,(\hbar^*/m^*)\,n_s^*(T)$, where L is the lenght of a strip, and is therefore proportional to $R_\square^{-1}(T_{co}-T)$ in the transition region [2].

Dynamical extensions of the KT theory [7] predict, near T_c, a drop in the real part (the superfluid component) and a peak in the imaginary part (the dissipative component) of $\varepsilon^{-1}(\omega,T)$. These characteristic features of the KT transition are clearly demonstrated by the experimental data of Fig. 1, where real and imaginary parts of the signal voltage δV, which is proportional to ε^{-1}, are shown as a function of temperature for a frequency of 70 kHz. These structures, which are quite similar to those observed in the dynamic response of other 2D systems [2,3], occur in a narrow ($\Delta T \simeq 20$ mK) critical region *below* $T_{co} = 1.992$ K, the temperature at which the dc resistance reaches half of its normal-state value.

Deeper insight into the nature of the phase transition is provided by a study of the temperature dependence of the helicity modulus, Γ, of the network. Γ is defined by [2,8] :

$$\Gamma = \varepsilon_b^{-1}(\ell_\omega)\,[1-(\tilde{T}/4)] \quad , \qquad (2)$$

where $\varepsilon_b(\ell_\omega)$ is the scale-dependent dielectric constant of the bound vortex pairs and the scale

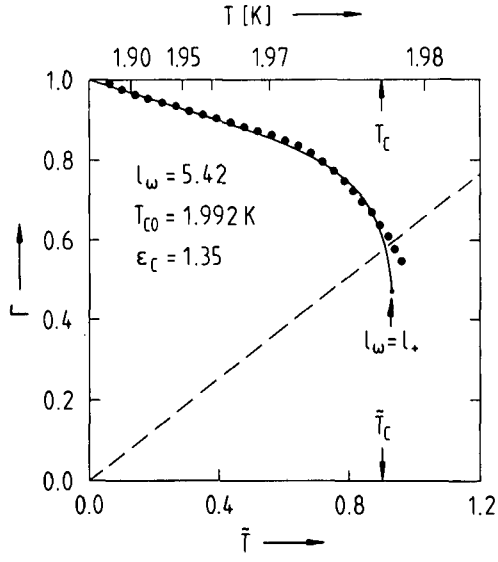

Fig. 2. Temperature dependence of the helicity modulus of a superconducting network deduced from its ac response (full circles) and as calculated from the KT theory (solid line). The dashed line is the KT universal prediction.

$\ell_\omega \equiv \ell n(r_\omega/a)$ is set by the size r_ω of those pairs which dominate the network response at the frequency ω [2,3,7]. In Eq.(2) $\tilde{T}$ is a dimensionless temperature defined by $\tilde{T} = 2ek_BT/\hbar i_c(T)$ [2,3] and the factor $[1-(\tilde{T}/4)]$ accounts for the renormalization of Γ due to spin-wave excitations [8]. Since $\varepsilon_b(\ell_\omega) = Re[\varepsilon(\omega,\tilde{T})]$ [2,7], $\Gamma(\tilde{T})$ can be extracted from the network response δV (Fig. 1) via Eq. (1). The result is shown in Fig. 2, along with a theoretical curve for $\Gamma(\tilde{T})$ obtained by numerically integrating the KT scaling equations [2]. In accordance with the theoretical prescription, the integration is truncated at a temperature $T_\omega > T_c$ such that $\ell_\omega = \ell_+$, where ℓ_+ is the scale corresponding to the free vortex correlation length above T_c[2,3].The overall agreement is excellent, considering there are only two adjustable parameters entering the calculation : $\varepsilon_c \equiv \varepsilon_b(\ell\to\infty, T_c)$ and N_0, a parameter related to the vortex configurational entropy [2]. From the fit of Fig.2 we infer $\varepsilon_c = 1.35$ and $N_0 = 0.2$. The dimensionless vortex unbinding temperature $\tilde{T}_c$ deduced from ε_c and the KT universal jump prediction $\Gamma(\tilde{T}_c) = (2/\pi)\tilde{T}_c$ is $\tilde{T}_c = 0.90$ (which leads to $T_c \cong 1.978$ K), a value very close to an estimate ($\tilde{T}_c \approx 0.91$) based on Monte Carlo simulations [9]. The small deviations of the data from the theoretical curve just above T_c is believed to arise from non-linear effects due to the small but non-vanishing driving current.

The ac response at 70 kHz of a wire network exposed to a perpendicular magnetic field $\vec{B}$ is shown in Fig. 3 as a function of $f = \phi/\phi_0$, the frustration parameter expressing the flux per unit cell $\phi = Ba^2$ in units of the superconducting flux quantum ϕ_0. Both components of δV show a complex oscillatory behaviour, the fundamental oscillation having a period of $f = 1$. As shown in the inset of Fig. 3, structures at odd half-integer values of f have also been resolved. Notice that the oscillations, which are observed only in a relatively narrow ($\Delta T \approx 30$ mK) temperature range below T_{c0}, persist out to fields as large as ~40 ϕ_0, indicating a high degree of sample homogeneity. The envelope of the signals is not fully understood at present,

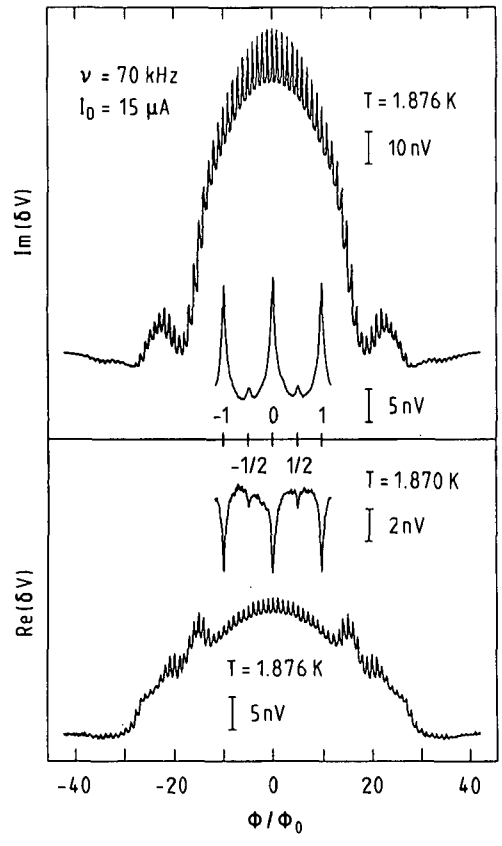

Fig. 3. Complex ac response of a superconducting network as a function of frustration $f = \phi/\phi_0$. Expanded view shows structure at f = 1/2.

although its main features are thought to result from the diffraction-like dependence of i_c on B in a single strip. The evolution of the ac response with temperature, partially revealed by the "dips" at T = 1.870 K and the "peaks" at T = 1.876 K in Re[$\delta V(f)$], is very similar to that observed in 2D arrays of SNS Josephson junctions [3] and can be qualitatively understood by considering the motion of a lattice of field-induced vortices with thermally activated defects in the periodic potential provided by the network.

This work was supported by the Swiss National Science Foundation.

REFERENCES

1) S. Teitel and C. Jayaprakash: J. Physique Lett. 46 (1985) L33.
2) J.E. Mooij: Percolation, Localization and Superconductivity, ed. A.M. Goldman and S.A. Wolf (Plenum, New York, 1984) NATO ASI SERIES Vol. B109, p. 325 and Refs. quoted therein.
3) Ch. Leemann, Ph. Lerch, G.-A. Racine and P. Martinoli: Phys. Rev. Lett. 56 (1986) 1291.
4) J.M. Kosterlitz and D.J. Thouless: J. Phys. C6 (1973) 1181.
5) R. Rammal, T.C. Lubensky and G. Toulouse: Phys. Rev. B27 (1983) 2820.
6) B. Pannetier, J. Chaussy and R. Rammal: Phys. Rev. Lett. 53 (1984) 1845.
7) V. Ambegaokar, B. I. Halperin, D.R. Nelson and E.D. Siggia: Phys. Rev. B21 (1980) 1806.
8) T. Ohta and D. Jasnow: Phys. Rev. B20 (1979) 139.
9) S. Teitel and C. Jayaprakash: Phys. Rev. B27 (1983) 598.

Solid State Communications, Vol. 71, No. 11, pp. 929-933, 1989.
Printed in Great Britain.

0038-1098/89$3.00+.00
Pergamon Press plc

ANISOTROPIC MICROWAVE ABSORPTION AND DC RESISTANCE IN MAGNETIC FIELDS OF GRANULAR SUPERCONDUCTING ALUMINUM FILMS

J.T. Suss*, W. Berlinger, A.M. Portis** and K.A. Müller

IBM Research Division, Zurich Research Laboratory, 8803 Rüschlikon, Switzerland

and

B. Jeanneret and P. Martinoli

University of Neuchâtel, Institute of Physics, 2000 Neuchâtel, Switzerland

(Received May 25th, 1989, by P. Wachter)

The microwave absorption and critical resistive behaviour of superconducting granular aluminum films, which are metallic in their normal state, have been examined. Microwave absorption is appreciable in these films and can be accounted for by dissipation of flux motion. Perpendicular flux readily penetrates the film while parallel flux enters more gradually. Film resistance is sensitive to field direction because of the perpendicular demagnetizing field, weak pinning of perpendicular flux and inhibited nucleation of parallel fluxons.

Introduction

GRANULAR aluminum films are extreme type-II superconductors[1] with transition temperatures T_c reported up to 3.74 K,[2] which are substantially higher than the critical temperature of bulk aluminum, $T_c = 1.183$ K. Microwave absorption and dispersion studies were first carried out in films of high resistivity[3] and gave evidence of their percolative character.[4,5] Experiments with a magnetic field perpendicular to the film were also reported.[6] This communication describes the results of microwave absorption of films in the metallic regime[3] in both low and high magnetic fields. In the present study microwave absorption and orientation dependence of the upper critical field H_{c_2} of granular aluminum films and anomalies were observed. The films appear to be microscopically isotropic without texture and with macroscopic anisotropy that results from (i) demagnetizing effects for magnetic fields normal to the plane of the film, (ii) pinning of perpendicular flux and (iii) inhibited nucleation of parallel flux. In earlier dc studies on other films, the presence of texture had been suggested.[3]

Films prepared by evaporating aluminum under reduced oxygen pressure[7] are composed of Al grains 30-40 Å in diameter or larger. The grain diameter increases at lower oxygen pressures and at increased rates of film deposition. Films with the largest grain diameters appear metallic with room-temperature resistivity below 100 $\mu\Omega$-cm. The resistivity of these films drops linearly with decreasing temperature. The superconducting transition temperature is a maximum for films with room-temperature resistivities around 100 $\mu\Omega$-cm. More highly oxidized films have lower transition temperatures and appear semiconducting with resistivities that increase with decreasing temperature.

Films were prepared by evaporating 99.99% pure Al onto suprasil substrates with the characteristics listed in Table 1. Film dimensions were length $L = 20$ mm, width $W = 3$ mm and thickness $t = 5500$ Å. Following Cohen and Abeles,[2] we take $\xi_0 = 8900$ and 9350 Å for samples 1 and 2, respectively, as the coherence length and $\lambda_L(0) = 157$ Å as the London penetration depth of an ideally clean film at $T = 0$. Within the dirty limit,[8] the coherence length near T_c is

$$\xi(T) = 0.855(\xi_0 \ell)^{1/2}/(1 - T/T_c)^{1/2} \qquad (1)$$

and the penetration depth is

$$\lambda_{\text{eff}}(T) = (\xi_0/1.33\,\ell)^{1/2}\,\lambda_L(0)/[2(1 - T/T_c)]^{1/2}. \qquad (2)$$

where ℓ is the effective mean free path. Calculated values of $\xi(0)$ and $\lambda_{\text{eff}}(0)$ as well as measured T_c's for two films are given in Table 1. For parallel fields the coherence length is sufficiently short for fluxons to nucleate to within 0.03 K of T_c.

Table 1. Film characteristics

Sample	ρ_{300}	T_c	ℓ	$\xi(0)$	$\lambda_{\text{eff}}(0)$
1	82 $\mu\Omega$-cm	2.12 K	20 Å	360 Å	2000 Å
2	56 $\mu\Omega$-cm	2.02 K	29 Å	430 Å	1700 Å

*Permanent address: Solid State Physics Department, Soreq Nuclear Research Center, Yavne 70600, Israel
**Permanent address: Department of Physics, University of California, Berkeley, CA 94720, USA

Films were immersed in liquid helium. Temperatures lower than 4.2 K were attained by reducing the vapor pressure of the liquid and monitored with a calibrated carbon-glass thermometer. The samples were placed along the narrow vertical edge of a TE_{102} K-band microwave cavity and allowed simultaneous observation of microwave absorption and determination of film resistance. Direct current flow along the length of the film was in the vertical direction, perpendicular to the plane in which the applied field H was rotated.

Areas of the film outside the microwave cavity had been overlaid with indium to which fine wires were soldered for four-terminal resistance measurements. The indium was found to contribute to the microwave absorption signal and had to be removed following the resistivity measurements for reliable microwave results up to the superconducting transition temperature of indium, $T_c = 3.408$ K.

Microwave Absorption

In contrast to the films with percolative character,[4,5] microwave absorption in the superconducting state of our films exposed to a magnetic field arises mainly from the oscillatory motion of fluxons driven by a microwave current density J_1 with a force per unit length

$$f = (1/c)\phi_0 J_1, \tag{3}$$

where $\phi_0 = hc/2e = 2.06786 \times 10^{-7}$ Gauss-cm^2 is the flux quantum. At microwave frequencies, pinning effects can be neglected[9] to a first approximation so that the absorption is simply proportional to the fluxon density $n = B/\phi_0$ and the fluxon velocity v,

$$dw/dt = n f v = nf^2/\eta, \tag{4}$$

where $\eta = v/f$ is the fluxon viscosity

$$\eta = \phi_0^2/\rho c^2 s \tag{5}$$

with ρ the normal-state resistivity. The moving fluxon induces dissipative currents that flow through a normal region which, in a homogeneous superconductor, is given by the area of the fluxon core $s = 2\pi\xi^2$. Because both the normal resistivity and the coherence length of granular films are large, the viscosity is low and the rate of energy absorption high. The absorption derivative has been obtained as a function of magnetic field and temperature with a K-band ($\nu \approx 20$ GHz) ESR spectrometer. Typically, the applied magnetic field, modulated at 120 Hz, is swept linearly from $H = 0$ or a slightly negative field to a maximum field and then linearly back to the starting field. In the earlier studies, the total microwave absorption was recorded.[4-6]

The forward and reverse traces of the absorption derivative in fields up to 100 Gauss are shown in Fig. 1(a) for a peak-to-peak field modulation amplitude $2H_m = 1$ Gauss. With the magnetic field normal to the plane of the film, the absorption derivative changes sign over a field interval of 5 Gauss as H is swept through zero-field. This sharp change in the derivative signal establishes that, in perpendicular fields, flux immediately fills the film. A similar behaviour has been observed in the microwave absorption in the ceramic cuprate superconductors.[10] However, in the metallic regime relevant to our case, sudden flux penetration is due to large demagnetizing effects for the perpendicular orientation of the field. In the ceramic superconductors, on the other hand, this results from the weak screening Josephson-like behaviour of this material. The reduction in signal with reversal of the field sweep is a consequence of flux pinning and is also observed in the high-temperature superconductors.[10] The displacement of the return trace by 0.5 Gauss indicates flux trapping by pinning. The absorption derivative shown in Fig. 1(b) for perpendicular fields up to 1000 Gauss with $2H_m = 30$ Gauss displays

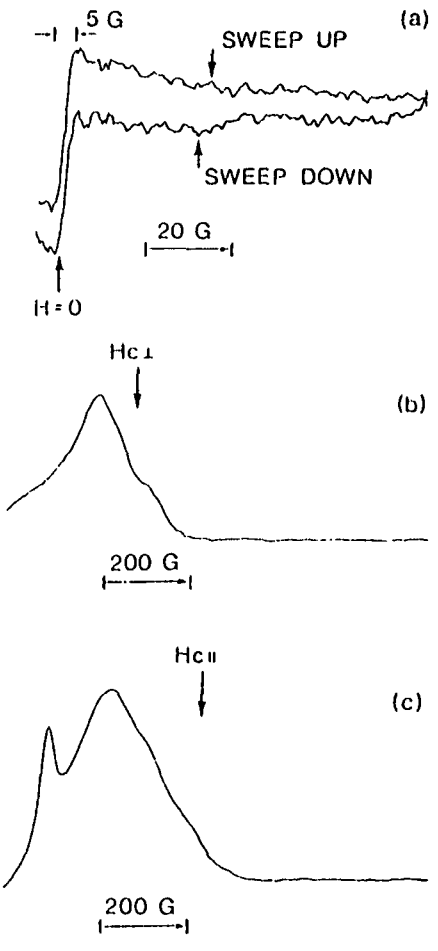

Fig. 1 (a) Modulated microwave absorption in low fields at $T \approx 1.98$ K with H perpendicular to the plane of the film. The field is swept from −4 to +100 Gauss and then back with a peak-to-peak (P-P) modulation field $2H_m = 1$ Gauss. (b) Modulated microwave absorption at $T = 1.9$ K with H perpendicular to the plane of the film. The field is swept from 0 to 1000 Gauss with a P-P modulation $2H_m = 30$ Gauss. $H_{c\perp}$ is indicated by an arrow. (c) Modulated microwave absorption at $T = 1.9$ K with H parallel to the plane of the film. The field is swept from 0 to 1000 Gauss with a P-P modulation $2H_m = 30$ Gauss. $H_{c\parallel}$ is indicated by an arrow.

the broad maximum that has been associated with a transition to the normal state.[5,10] The maximum in the absorption derivative is broad at the lowest temperatures and narrows in field, becoming more asymmetric at higher temperatures. Hysteresis in the maximum with sweep direction gives further evidence of flux pinning. The position of the maximum approaches zero-field linearly with increasing temperature as shown in Fig. 2. This is the behaviour expected[8] for the upper critical field H_{c_2} near T_c

$$H_{c_2}(T) = \phi_0/2\pi\xi(T)^2. \quad (6)$$

Using the parameters in Table 1, calculated values of $-dH_{c_2}/dT$ for films 1 and 2 are 2530 Gauss/K and 1660 Gauss/K. The variation in H_{c_2} inferred from the resistive transition of sample 2 is larger (see Fig. 2).

With the magnetic field nominally parallel to the plane of the film, a similar broad maximum in the absorption derivative is obtained as shown in Fig. 1(c). In addition, a narrow maximum is observed around 100 Gauss. This narrow maximum, which is not observed in perpendicular fields, may be associated with fluxon nucleation in parallel fields, which is consistent with the nucleation condition $d < \xi(T)$.[8]

The microwave absorption derivative has also been measured with a dc current through the film and H parallel and perpendicular to the plane of the film. For current densities up to 4800 A/cm^2 the microwave absorption derivative was unaffected by the current. We conclude that even though currents in this range affect flux flow, there is no effect on the density of flux penetrating the film.

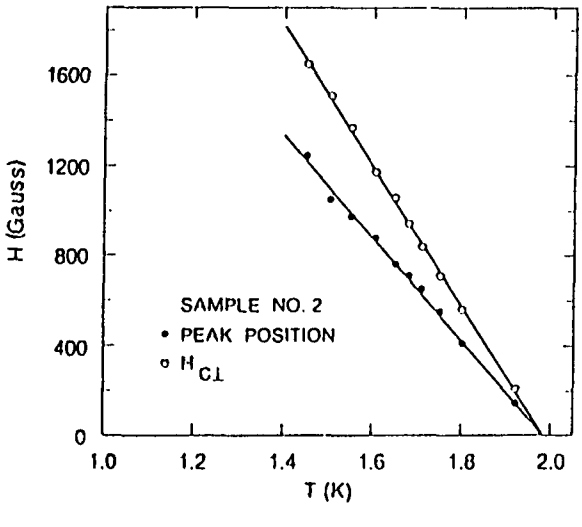

Fig. 2. Temperature dependence of the perpendicular field at which the microwave absorption derivative is a maximum. For comparison, the perpendicular field $H_{c\perp}$ is shown at which the resistivity reaches half its normal value. The solid lines are best fits for the temperature dependence of the maximum and $H_{c\perp}$, respectively.

Resistance to Current Flow

Low-Field Resistance

With a magnetic field applied to the film, fluxons that are depinned by currents generate film resistance *at current densities well below the depairing value*. The voltage recorded between terminals in low magnetic fields is shown in Fig. 3. The behaviour of the voltage at low current, $J = 1.5$ A/cm^2, through the film and H normal to the film at $T = 1.76$ K, substantially below T_c, is shown in Fig. 3(a). At these low current densities the voltage rises only slowly with magnetic field. This behaviour is common[10] and results from the depinning of flux above a current-density threshold

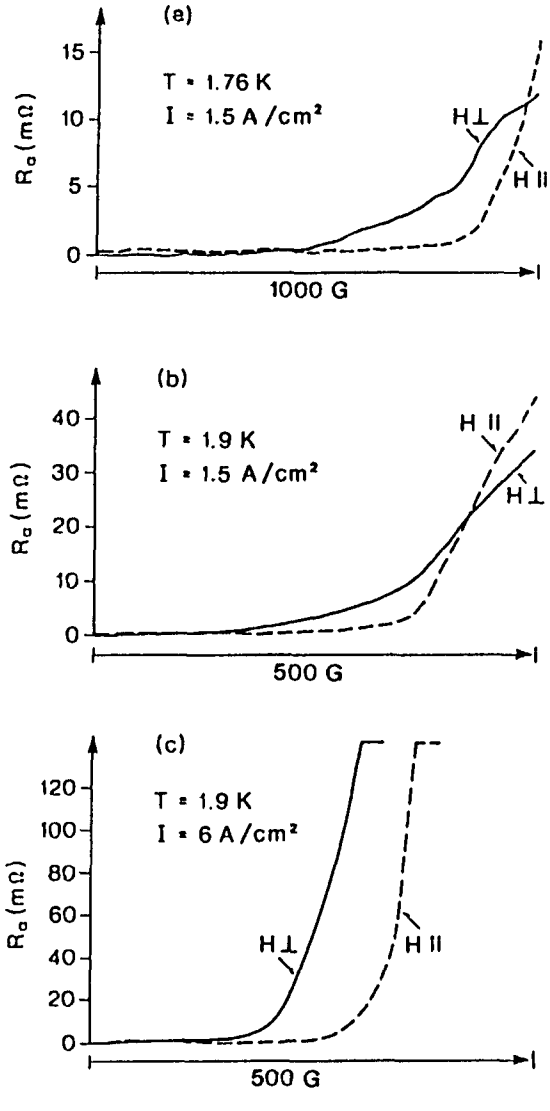

Fig. 3. Comparison of the dc sheet resistance $R = (W/L)(V/I)$ as a function of the applied magnetic field H in low fields parallel and perpendicular to the plane of the film at the following temperatures and with the following current densities: (a) T = 1.76 K, J = 1.5 A/cm^2, (b) T = 1.90 K, J = 1.5 A/cm^2, (c) T = 1.90 K, J = 6.0 A/cm^2.

that decreases with increasing fields.[11] With the magnetic field in the plane of the film, a threshold field appears to be observed for the development of a voltage across the film.

The voltage recorded at a slightly higher temperature $T = 1.90$ K and at the same current density $J = 1.5$ A/cm^2 is shown in Fig. 3(b). Raising the temperature reduces the threshold field for H parallel to the surface. Above this threshold, the parallel resistance $R_\parallel$ rises rapidly and may exceed the perpendicular resistance $R_\perp$. The slower rise in $R_\perp$ is believed to result from pinning, which reduces the rate at which perpendicular flux flows into the film. $R_\parallel$ can rise more rapidly because parallel flux need cross only the much shorter thickness of the film.

The voltage recorded at the same temperature $T = 1.90$ K and at a higher current density $J = 6.0$ A/cm^2 is shown in Fig. 3(c). At higher current densities, the voltage in perpendicular field rises at an increased rate. However, as long as the field is accurately parallel to the surface of the film, increasing the current does not appreciably reduce the apparent critical field.

The extracted dc sheet resistance $R = (W/L)(V/I)$ as a function of current density J at $T = 1.95$ K is shown in Fig. 4 for magnetic fields H from 50 to 250 Gauss. We first characterize the perpendicular field behaviour shown in Fig. 4(a). The sheet resistance R appears to approach saturation for currents in excess of 60 A/cm^2 at fields H above 100 Gauss. The linear response in R for low J, which is equivalent to an increase in V that is quadratic with J, results from a uniform distribution $B(J_c)$ of flux as a function of critical current density.[11]

The low-field sheet resistance R for parallel fields shown in Fig. 4(b) is similar to that for perpendicular fields except that because of the presence of a threshold field. The fields required for the development of the resistance are substantially higher. At higher magnetic fields and low currents the voltage V increases more rapidly for H parallel than for H perpendicular to the plane of the film because flux pinning limits the flow of perpendicular flux into the film more than it does parallel flux. An important difference between Figs. 4(a) and (b) is that the sheet resistance climbs more slowly with current in the same magnetic field for H parallel to the surface than for H perpendicular. Reduced resistance with H parallel to a surface has been carefully studied by Swartz and Hart[12] and attributed to a surface barrier for the nucleation of parallel flux.

High-Field Resistance

At high flux densities, $R_\perp$ and $R_\parallel$ first become independent of current and ultimately independent of magnetic field, as the film goes into the normal state. The field $H_{c\perp}$ at which $R_\perp$ reaches half the normal value R_n is plotted in Fig. 2 for comparison with the temperature-dependence of the maximum in the microwave absorption derivative. The field $H_{c\parallel}$ at which $R_\parallel$ reaches $0.5\,R_n$ is somewhat larger.

Reduced resistivity in the plane of a film at temperatures below T_c is expected from the equilibrium superconducting surface sheet proposed by Saint-James and de Gennes.[13]

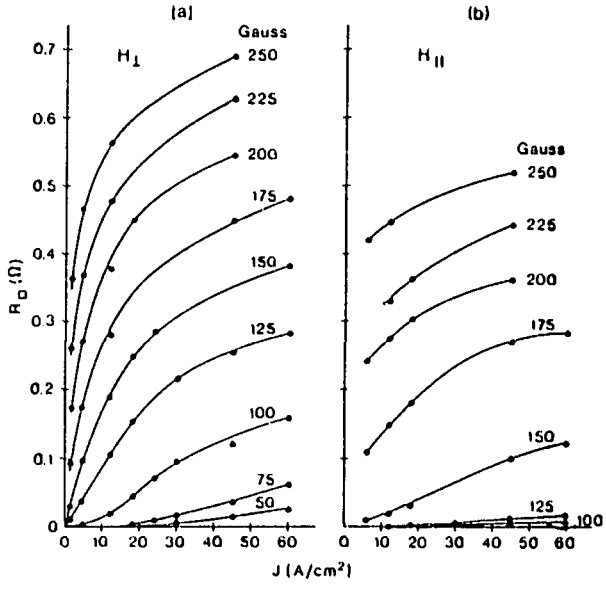

Fig. 4. Plot of the sheet resistance $R = (W/L)(V/I)$ in various magnetic fields H as a function of the current density J. (a) Measurement with the magnetic field H normal to the plane of the film. (b) Measurement with the magnetic field in the plane of the film and normal to the direction of current flow. T = 1.95 K.

Summary and Conclusions

The observed microwave absorption derivative of granular aluminum films in the metallic regime is consistent with an effective-medium model with a normal-state resistivity ρ_n, a coherence length $\xi(T)$ and a penetration depth $\lambda_{eff}(T)$ that increase as T approaches T_c. The broad absorption derivative maximum observed in perpendicular fields marks the transition to the normal state. An additional narrow maximum observed only in parallel fields may be associated with the nucleation of flux lines. The absorption is insensitive to dc current and establishes the findings that current has little effect on flux penetration.

The properties of granular films in the resistive state are sensitive to the nucleation and trapping of flux. Flux flow is observed to depend in a complex way on field, temperature and current, and is sensitive to the orientation of the field with respect to the plane of the film. Measurements of the dependence of the sheet resistance on current and magnetic field convince us that the observed anisotropy arises from macroscopic effects — demagnetizing fields, weak pinning, and a possible surface barrier to the nucleation of fluxons.

Determinations of H_{c_1} in thin single crystals of $YBa_2Cu_3O_{7-\delta}$ by resistive methods may be similarly sensitive to flux flow for applied fields parallel and perpendicular to the conducting ab planes. Magnetic measurements are a way to avoid such problems.[14,15]

REFERENCES

1. For a historical introduction see M. Tinkham in *Inhomogeneous Superconductors – 1979*, edited by D.U. Gubser, T.L. Francavilla, S.A. Wolf & J.R. Leibowitz, AIP Conference Proceedings No. 58, p. 1, American Institute of Physics, New York (1980).
2. R.W. Cohen & B. Abeles, *Phys. Rev.* **168**, 444 (1968).
3. G. Deutscher & S.A. Dodds, *Phys. Rev. B* **16**, 3936 (1977).
4. K.A. Müller, M. Pomerantz, C.M. Knoedler & D. Abraham, *Phys. Rev. Lett.* **45**, 832 (1980).
5. E. Stocker & J. Bullet, *Solid State Commun.* **53**, 915 (1985); E. Stocker, Ph.D. Thesis, EPFL Lausanne, Switzerland (1984).
6. M. Pomerantz & K.A. Müller, *Physica* **107B**, 325 (1981).
7. G. Deutscher, H. Fenichel, M. Gershenson, E. Grünbaum & Z. Ovadyahu, *J. Low Temp. Phys.* **10**, 231 (1973).
8. M. Tinkham, *Introduction to Superconductivity*, McGraw-Hill Inc., New York (1975).
9. J.I. Gittleman & B. Rosenblum, *Phys. Rev. Lett.* **16**, 734 (1966).
10. K.W. Blazey, A.M. Portis & J.G. Bednorz, *Solid State Commun.* **65**, 1153 (1988).
11. J.P. Burger, G. Deutscher, E. Guyon & A. Martinet, *Phys. Rev.* **137**, A853 (1965).
12. P.S. Swartz & H.R. Hart, Jr., *Phys. Rev.* **137**, A818 (1965).
13. D. Saint-James & P.G. de Gennes, *Phys. Lett.* **7**, 306 (1963).
14. W.J. Gallagher, T.K. Worthington, T.R. Dinger, F. Holtzberg, D.L. Kaiser & R.L. Sandstrom, *Physica* **148B**, 228 (1987).
15. A. Umezawa, G.W. Crabtree, J.Z. Liu, T.J. Moran, S.K. Malik, L.H. Nunez, W.L. Kwok & C.H. Sowers, *Phys. Rev. B* **38**, 2843 (1988).

PHYSICAL REVIEW B VOLUME 40, NUMBER 16 1 DECEMBER 1989

Critical phase fluctuations in superconducting wire networks

B. Jeanneret, Ph. Flückiger, J. L. Gavilano, Ch. Leemann, and P. Martinoli
Institut de Physique, Université de Neuchâtel, 2000 Neuchâtel, Switzerland
(Received 21 September 1989)

A study of the onset of superconducting phase coherence in periodic wire networks with weakly coupled adjacent nodes is presented. In a narrow temperature range below the mean-field critical temperature, ac conductance measurements reveal a drop in superfluid density and a peak in dissipation providing the first observation in networks of the vortex unbinding transition predicted by the Kosterlitz-Thouless theory. The ac response in the critical region is accurately described by dynamical extensions of the theory incorporating vortex-pinning phenomena created by the periodic structure of the network.

Networks of superconducting wires and arrays of Josephson weak links[1] prepared by modern lithographic techniques provide excellent systems to study fundamental concepts of condensed matter and statistical physics. Particularly attractive is the possibility of using these systems as testing grounds for the theoretical ideas of scaling, renormalization, frustration, and randomness underlying the physics of critical phenomena in two dimensions.

In this paper we explore the nature of the superconducting-to-normal (SN) transition (in zero magnetic field) of periodic two-dimensional (2D) wire networks[2] in the limiting case of weakly coupled nearest-neighbor nodes. Relying on a two-coil mutual-inductance method[3] to study the ac superfluid response of the system to a small oscillating driving field, we observe features in the critical region which provide strong evidence for a phase transition triggered by the vortex unbinding mechanism of the Kosterlitz-Thouless (KT) theory.[4] This conclusion is corroborated by a detailed study of the response based on dynamical extensions[5] of the KT theory. An important and distinctive aspect of our experiments, the fluctuating Brownian motion of vortex excitations in the periodic pinning potential created by the network, was included in the theoretical treatment and is shown to have a profound effect on the characteristic length scales probed in the ac measurements. The quality of the fit between theory and experiment emerging from our analysis is remarkable, comparable to that found so far only in studies of the superfluid transition in liquid-helium films[6] and in indium oxide films.[7] The results presented here are the first to show the KT transition in a network of superconducting wires. Previous work[2] on this system was performed in the strong-coupling regime, where the phase boundary in the (H,T) plane was found to be accurately described by the mean-field Ginzburg-Landau (GL) theory.

The nature of the SN transition of wire networks depends on the ratio a/ξ between the network lattice spacing a and the GL coherence length $\xi(T)$. Inspection of the GL free energy of the system[8] shows that for $a \ll \xi$ Josephson coupling between adjacent nodes is strong, the coupling energy being a factor $(2\xi/a)^2$ larger than the condensation energy in the interconnecting link. In this limit fluctuations in the phase ϕ_i of the complex order parameter at the nodal sites are irrelevant and the SN phase boundary of the network in the (H,T) plane is obtained by solving a linearized GL equation.[2]

The critical behavior of weakly coupled $(a \gg \xi)$ wire networks is radically different from that predicted by the mean-field GL approach. In this regime, below the mean-field critical temperature T_{co}, 2D phase fluctuations are essential to determine the nature of the SN transition, while amplitude fluctuations can be ignored. Assuming a position-independent order-parameter amplitude, which appears to be justified for $a \gg \xi$, the coupling energy of nearest-neighbor nodes takes on the piecewise parabolic dependence on $(\phi_i - \phi_j)$ characteristic of long $(a \gg \xi)$ microstrips with a piecewise linear current-phase relation.[9] The resulting expression of the free energy[8] shows that weakly coupled wire networks belong to the class of classical XY models with a temperature-dependent coupling energy given by[9]

$$E_J(T) = (\pi/4)(R_u/R_s)\Delta(T)\tanh[\Delta(T)/2k_BT] ,$$

where $\Delta(T)$ is the BCS gap parameter, R_s the normal-state strip resistance, and $R_u = \hbar/e^2$. According to the KT theory, the (zero field) critical behavior of the system is governed by 2D-phase fluctuations in the form of quantized vortices, the transition to the resistive state being driven by the unbinding of vortex-antivortex pairs at a critical temperature T_c lower than T_{co}.[9]

To ascertain this prediction, square wire networks with $a = 8$ μm containing about 10^6 nodes were photolithographically patterned from 200-Å-thick granular aluminum films. An appreciable reduction of T_c below T_{co} $(T_{co} - T_c \approx 100$ mK) and an $a/\xi(T_c)$ ratio of the order of 100 were obtained by an appropriate choice of the strip width $(w \approx 0.8$ μm) and of the normal-state resistivity of the Al films $(\rho \approx 150$ $\mu\Omega$ cm). The onset of 2D superconducting phase coherence in the networks was probed by studying their ac screening properties with an inductive technique.[3] The method consists of exposing the network to a weak ac magnetic field created by a 4-mm-diam drive coil located just above the sample. The excitation level, chosen to ensure a linear response, reached a maximum rms value of ~ 0.4 mG at the center of the network, while ambient magnetic fields were suppressed to ~ 1 mG. The response of the sample to the ac field was measured by

detecting the in-phase and quadrature components of the signal δV induced by the screening currents in a pair of astatic 2-mm-diam coils coaxially mounted within the drive coil. Data were taken at angular frequencies ω ranging from $\sim 6\times 10^3\ s^{-1}$ to $\sim 6\times 10^7\ s^{-1}$.

Figure 1 shows, emphasizing the critical-temperature region, the complex ac response $\delta V(T)$ measured at 10, 65, and 1000 kHz of an Al network with $R_s = 750\ \Omega$. Since the weak screening condition is almost satisfied at the temperatures of interest, $\delta V(T)$ is, to a first approximation, proportional to the complex ac conductance $G(T)$ of the sample.[3] In particular, $\mathrm{Im}[\delta V(T)]$ reflects the temperature dependence of the inverse kinetic inductance $L_K^{-1}(T)$ which measures the effective (renormalized) areal superfluid density in the network.[9] As shown in Fig. 1, in a narrow temperature range ($\Delta T \approx 30$ mK) centered about a frequency-dependent critical temperature T_ω we observe a marked drop in superfluid density, while a peak, whose position is used to locate T_ω, grows in the dissipative part $\mathrm{Re}[\delta V(T)]$ of the signal. These features are quite similar to those observed in ac measurements of the superfluid transition of other 2D systems[6,7,10,11] and as discussed in detail below, can be accurately described by dynamical theories[5] based on the KT vortex unbinding idea.

Also shown in Fig. 1 (upper part) is the dc resistive transition of the network. On the high-temperature side above T_{co}, fluctuations in the order-parameter amplitude lower the network sheet resistance below its normal-state value R_s. To obtain an estimate of T_{co}, the inverse excess conductance $(R^{-1}-R_s^{-1})^{-1}$ was fitted to the Aslamasov-Larkin theory[12] for fluctuation-induced superconductivity in two dimensions using T_{co}, R_s, and R_u as adjustable parameters.[7] From the fit, shown in the lower part of Fig. 1, we deduce $T_{co} = 2.236$ K, $R_s = 750\ \Omega$, and $R_u = 4.94\ \mathrm{k}\Omega$ (the theoretical value of R_u is 4.11 kΩ). The uncertainty in the determination of T_{co} is 25 mK.

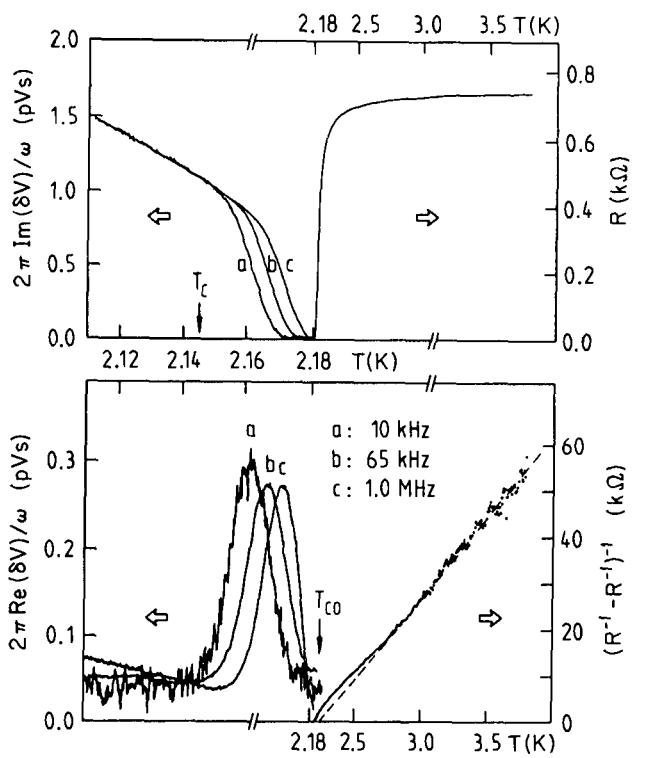

FIG. 1. Complex ac response vs temperature of a weakly coupled wire network measured at different frequencies near the superconducting transition. Also shown are the resistive transition (upper part) and the inverse excess conductance above T_{co} (lower part). The dashed line is a fit to the Aslamasov-Larkin theory.

The quantity to be compared with theory is the complex ac conductance rather than the signal voltage. Accordingly, G was calculated from the δV data by numerically solving the integral equation relating δV to G for our specific sample-coil configuration.[3] An example is shown in Fig. 2, where real and imaginary parts of ωG, as deduced from the 65-kHz response of Fig. 1, are plotted as a function of temperature and compared with the following prediction of the dynamical theory:[5,9]

$$G^{-1}(T,\omega) = [\omega L_{K0}(T)/\tilde{T}][\pi^4 y^2(l_\omega,\tilde{T}) + iK^{-1}(l_\omega,\tilde{T})] + R(\tilde{T})[a/\xi_+(\tilde{T})]^2, \quad (1)$$

where $L_{K0}(T) = (\hbar/2e)^2/E_J(T)$ is the kinetic inductance in the absence of thermal fluctuations. Equation (1) shows the decomposition of the network impedance G^{-1} in contributions from bound vortex pairs and from free vortices. The complex vortex-pair contribution is expressed in terms of two scale-dependent $[l \equiv \ln(r/a)]$ and temperature-dependent $[\tilde{T} \equiv k_B T/E_J(T)]$ quantities: the reduced stiffness K and the vortex excitation probability y. The characteristic length scale probed in the ac measurements is the vortex diffusion length $r_\omega \approx (14\mu k_B T/\omega)^{1/2}$, where μ is the vortex mobility discussed below in connection with thermally activated vortex motion in the periodic potential provided by the network. The renormalization procedure based on the Kosterlitz recursion equations[9,13] allows K and y to be computed for $l = l_\omega$ once their initial values at $l = 0$ are known. Adopting Mooij's notion,[9] we take $K(0,\tilde{T}) = \tilde{T}^{-1}$ and $y(0,\tilde{T}) = N_0 \exp(-2\pi\gamma/\tilde{T})$,

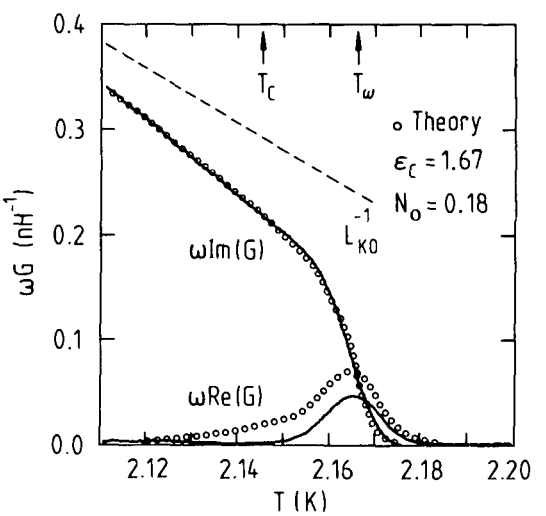

FIG. 2. Experimental (solid curves) and theoretical (open circles, see text) complex ac conductance at 65 kHz of the network of Fig. 1 as a function of temperature near the superconducting transition. The dashed line is the GL mean-field prediction.

where N_0 and γ are nonuniversal parameters related to the vortex-core energy. Above T_c, the theoretical prescription $y(l_+,\tilde{T})=y(0,\tilde{T})$ for truncating the renormalization process introduces a new length scale, the correlation length $\xi_+(\tilde{T})\equiv ae^{l_+(\tilde{T})}$ which measures the average distance between free vortices.

Unlike vortex excitations in ideal superconducting films, vortices in networks experience the pinning effect due to the underlying periodic structure. Using a continued-fraction method, it is possible to estimate the ac vortex mobility in networks by studying the Brownian motion of an individual vortex exposed, for simplicity, to a sinusoidal force field.[14] At the low frequencies used in our experiments, the result is

$$\mu(T)=(a/\phi_0)^2R(T)=(a/\phi_0)^2R_s[I_0(U/2k_BT)]^{-2};$$

where $I_0(x)$ is the modified Bessel function of order zero and U the potential barrier created by the interconnecting links. To estimate the activation energy, we observe that in the critical region the strip width is such that $w/\xi\gg 1$ [typically, $w/\xi(T_\omega)\approx 10$], thereby requiring the nucleation of a normal vortex core during the link crossing process.[15] Thus, U will be almost entirely determined by the condensation energy associated with the core nucleation process. Using Clem's vortex model,[16] we find $U/2k_BT\approx(\pi a/4w)\tilde{T}^{-1}$. In our networks the a/w ratio is so large ($a/w\approx 10$) that, because of the exponential character of $I_0(x)$ for $x\gg 1$, $\mu(T)$ drops by several orders of magnitude in a narrow temperature range below T_{co}, thereby causing the drastic reduction of l_ω which accounts for the observed broadening of the transition. At sufficiently low temperatures, however, vortex pinning and vortex-vortex correlations become so strong that a model based on the Brownian motion of a single vortex excitation is no longer appropriate and the theory is expected to fail. A manifestation of this failure is the "reentrant" behavior of Re$[G(T)]$ (not shown in Fig. 2) predicted by the model below a certain temperature $T^*<T_\omega$ ($T^*\approx 2.15$ K in Fig. 2). The origin of this unphysical feature can be traced back to the very short length scales entering renormalization for $T<T^*$. This suggests interpreting the characteristic length at T^*, $r_\omega(T^*)$, as the shortest length scale consistent with the model. Accordingly, in the calculations presented below, $l_\omega(T)$ was kept fixed at $l_\omega(T^*)$ for $T<T^*$ [$l_\omega(T^*)\approx 0.8$ in Fig. 2].

Setting $U/2k_BT\approx\alpha\tilde{T}^{-1}$, the ac conductance data of Fig. 2 were fitted to Eq. (1) using N_0, α, γ, and T_{co} as adjustable parameters (R_s was kept at 750 Ω). An excellent fit of the inductive component is obtained for $N_0=0.18$, $2\pi\gamma=0.82$, $\alpha=7.85$, and $T_{co}=2.258$ K, while the computed dissipative component sets in at temperatures too low to agree with the data. However, considering the high sensitivity of the response to vortex pinning and the approximate method used to incorporate its effect in the dynamical theory, we feel that dissipation is, on the whole, remarkably well described by our model. The value of α is in very good agreement with the predition of Clem's model, whereas T_{co} is consistent with the result extracted from the paraconductivity contribution to the dc conductance above T_{co}. Using α and T_{co} as deduced from the fit, we can estimate the typical length scales explored at 65 kHz: we find $l_\omega=1.13$ ($r_\omega=3.1a$) at $T_\omega=2.166$ K. From the expression relating N_0 and γ to the vortex dielectric constant ϵ_c (Ref. 9) we find $\epsilon_c=1.67$, a value in good agreement with the result ($\epsilon_c\approx 1.70$) of Monte Carlo simulations.[17] Finally, from the universal prediction $K^{-1}(\infty,\tilde{T}_c)=\epsilon_c\tilde{T}_c=\pi/2$ we obtain $T_c=2.146$ K.

As demonstrated by the data of Fig. 1 and predicted by the dynamical theory, the vortex unbinding transition shifts to higher temperatures with increasing ω. If one identifies T_ω as the temperature where the crossover from a vortex-pair- to a free-vortex-dominated response occurs, then T_ω is implicitly defined by $r_\omega(\tilde{T}_\omega)\approx\xi_+(\tilde{T}_\omega)$.[5] To test this fundamental prediction, $r_\omega(\tilde{T}_\omega)$ was deduced from the measured T_ω, while $\xi_+(\tilde{T})$ was computed from the theoretical prescription $y(l_+,\tilde{T})=y(0,\tilde{T})$. All calculations were consistently performed with the parameter values which fit the data of Fig. 2. The results, expressed in terms of the dimensionless quantities l_ω^{-2} and l_+^{-2}, are shown in Fig. 3 as a function of the reduced-temperature shift $(\tilde{T}_\omega-\tilde{T}_c)$. For small shifts (low ω) the scaling parameter inferred from experiment (l_ω) is in excellent agreement with theory (l_+), whereas deviations from the predicted behavior occur for large shifts of T_ω (high ω). This might be due to the fact that the KT theory is less accurate at temperatures well above T_c. Figure 3 also shows that the large length scales required to explore the region very close to T_c were not accessible in our experiments. In this temperature range $l_+^{-2}(\tilde{T})$ is predicted[4,13] to assume the asymptotic form $l_+^{-2}=b(\tilde{T}-\tilde{T}_c)$. If b is consistently computed[9] from N_0 and ϵ_c ($b=0.51$), the data cannot be fitted by this expression, which is obeyed only in a very narrow (~2 mK) interval just above T_c. In light of this result, evidence for the square-root singularity of $l_+(\tilde{T})$ found in previous work[9,10] should be reconsidered.

In conclusion, measurements of the complex ac conductance of weakly coupled superconducting wire networks

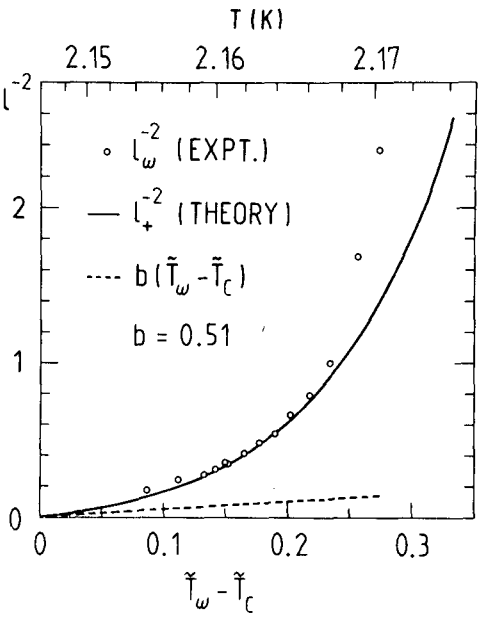

FIG. 3. Dependence of the scaling parameter l_ω on the shift of the dimensionless vortex-unbinding temperature $\tilde{T}_\omega$. The solid line is the prediction of the dynamical KT theory, the dashed line its asymptotic form very close to T_c.

have provided the first observation of the Kosterlitz-Thouless vortex unbinding transition in this system. The remarkable degree of quantitative agreement emerging from the theoretical analysis of the dynamic response suggests that weakly coupled wire networks will also be ideal model systems for studies of critical phenomena in frustrated and/or disordered two-dimensional systems. Apart from their intrinsic fundamental importance, such investigations should provide a deeper understanding of some of the intriguing magnetic properties of high-temperature superconducting ceramics.

We would like to thank H. Beck for many stimulating discussions and U. Mohr, D. Varidel, and Y. Oppliger for technical assistance. This work was supported by the Swiss National Science Foundation.

[1]For a recent review of the field, see *Coherence in Superconducting Networks,* edited by J. M. Mooij and G. B. J. Schön [Physica B **152**, Nos. 1 and 2 (1988)].

[2]B. Pannetier, J. Chaussy, R. Rammal, and J. C. Villegier, Phys. Rev. Lett. **53**, 1845 (1984).

[3]A. T. Fiory and A. F. Hebard, in *Inhomogeneous Superconductors—1979,* edited by D. U. Gubser, T. L. Francavilla, S. A. Wolf, and J. R. Leibowitz, AIP Conf. Proc. No. 58 (American Institute of Physics, New York, 1979), p. 293; A. T. Fiory, A. F. Hebard, P. M. Mankiewich, and R. E. Howard, Appl. Phys. Lett. **52**, 2165 (1988); B. Jeanneret, J. L. Gavilano, G. A. Racine, Ch. Leemann, and P. Martinoli, Appl. Phys. Lett. (to be published).

[4]J. M. Kosterlitz and D. J. Thouless, J. Phys. C **6**, 1181 (1973).

[5]V. Ambegaokar, B. I. Halperin, D. R. Nelson, and E. D. Siggia, Phys. Rev. B **21**, 1806 (1980); S. R. Shenoy, J. Phys. C **18**, 5163 (1985).

[6]D. J. Bishop and J. D. Reppy, Phys. Rev. B **22**, 5171 (1980).

[7]A. T. Fiory, A. F. Hebard, and W. I. Glaberson, Phys. Rev. B **28**, 5075 (1983).

[8]S. Teitel and C. Jayaprakash, J. Phys. (Paris) Lett. **46**, L33 (1985).

[9]J. E. Mooij, in *Percolation, Localization and Superconductivity,* edited by A. M. Goldman and S. A. Wolf (Plenum, New York, 1984), p. 325.

[10]Ch. Leemann, Ph. Lerch, G.-A. Racine, and P. Martinoli, Phys. Rev. Lett. **56**, 1291 (1986).

[11]A. T. Fiory, A. F. Hebard, P. M. Mankiewich, and R. E. Howard, Phys. Rev. Lett. **61**, 1419 (1988).

[12]L. G. Aslamasov and A. I. Larkin, Fiz. Tverd. Tela. **10**, 1104 (1968) [Sov. Phys. Solid State **10**, 875 (1968)].

[13]J. M. Kosterlitz, J. Phys. C **7**, 1046 (1974).

[14]P. Martinoli, M. Nsabimana, G.-A. Racine, H. Beck, and J. R. Clem, Helv. Phys. Acta **56**, 765 (1983).

[15]K. K. Likharev, Rev. Mod. Phys. **51**, 101 (1979).

[16]J. R. Clem, J. Low Temp. Phys. **18**, 427 (1975).

[17]S. Teitel and C. Jayaprakash, Phys. Rev. B **27**, 598 (1983).

Inductive conductance measurements in two-dimensional superconducting systems

B. Jeanneret, J. L. Gavilano, G. A. Racine, Ch. Leemann, and P. Martinoli
Institut de Physique, Université de Neuchâtel, CH-2000 Neuchâtel, Switzerland

(Received 25 August 1989; accepted for publication 29 September 1989)

A two-coil mutual-inductance technique for measuring the complex ac response of a two-dimensional (2-D) superconductor to a weak ac magnetic field is described. Analytical and numerical methods are presented which allow extraction of the complex ac conductance of the superconductor from the signal voltage induced in the detection coil by the screening currents flowing in the sample. The method is illustrated by measurements of the ac conductance of a square network of aluminum wires from which the penetration depths of both the network and (granular) aluminum are deduced. It is shown that the method provides a powerful tool to observe characteristic features associated with critical phenomena in 2-D superconducting systems.

The response of a superconductor to time-dependent electromagnetic fields can be described in terms of the complex ac conductivity of the system. Conductivity measurements probe the dynamics of the accelerated superfluid and of low-energy excitations from the superconducting ground state such as quasiparticles and vortices. A particularly attractive aspect of experiments focusing on the ac conductivity is the possibility to perform accurate measurements of a fundamental parameter of superconductivity, the magnetic penetration depth, and to explore in detail the nature of various dissipative processes.

A two-coil mutual-inductance technique for measuring the low-frequency complex sheet conductance (rather than the ac conductivity) of two-dimensional (2-D) superconductors was first devised by Fiory and Hebard,[1] who used it to study thin films of aluminum/aluminum-oxide[2] and indium/indium-oxide composites[3] and, recently epitaxial YBaCuO layers.[4] In recent work, we used a modified version of Fiory–Hebard's method to investigate magnetic screening and dissipation in connection with critical phenomena in 2-D arrays of proximity effect Josephson junctions,[5] in 2-D wire networks[6] and in granular high T_c films.[7] In consideration of the current widespread interest in thin films of the novel superconducting oxides, in this letter we give a thorough account of our drive-receive coil technique which has been only marginally described in previous work. Relying on accurate control of the two-coil geometry to model ac currents and fields, we derive an *analytical* expression relating the signal voltage δV at the receiver to the ac sheet conductance G of the sample. This distinctive aspect of our method favors the use of a very simple yet powerful numerical inversion procedure[4] to extract G from δV, thereby providing detailed insight into the physics of 2-D superconductors.

At the heart of the ac conductance measuring system, shown in Fig. 1, there are a drive coil of radius $R_D = 2.05$ mm and a pair of astatically wound receive coils of radius $R_R = 1.2$ mm coaxially mounted within the excitation coil. Mechanical stability is achieved by embedding the coil assembly in stycast. The drive coil has $N_D = 23$ turns equally spaced by $\delta h_D = 0.2$ mm, and is placed at a distance h_D of 0.3 mm from the sample. The two mutually compensating sections of the detection coil have $N_R = 15$ turns each of 20-μm-diam wire, the uniform spacing δh_R between the turns being the only adjustable parameter used in the calibration procedure outlined below (δh_R is of the order of 30 μm). The gradiometer configuration of the receiver favors sensitivity to currents flowing in the film with respect to those circulating in the drive coil and helps to suppress external flux noise. To achieve maximum sensitivity, the distance h_R of the lower detection coil to the sample is kept as small as possible (h_R is at least an order of magnitude smaller than h_D). The in-phase and quadrature components of the voltage δV at the receive coil due to the screening currents flowing in the superconducting sample in response to an ac current of amplitude I_D and angular frequency ω in the drive coil are detected by conventional lock-in techniques or by an ac mutual-inductance bridge incorporating a superconducting quantum interference device (SQUID) detector. To illustrate our method we present conductance measurements performed on a network of aluminum wires[6] of width $w = 1.4\,\mu$m forming a square lattice with 10^6 nodes connected by strips of length $a = 8\,\mu$m and normal-state resistance

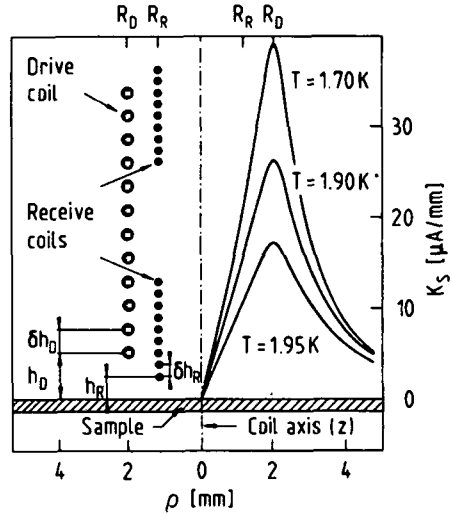

FIG. 1. Left side: geometry of the drive-receive coil system. Right side: radial sheet current density distribution in a superconducting network of Al wires as computed from Eq. (4) for three different temperatures ($I_D = 15$ μA).

 0003-6951/89/482336-03$01.00

$R_s = 95\ \Omega$. The sample was patterned from a 400-Å-thick granular Al film using standard photolithography and wet etching.

To study the response of the superconducting system to the ac magnetic field created by the drive coil, we first derive an expression for the sheet current density $\mathbf{K}_s$ in the sample, which is assumed to be homogeneous and isotropic over the characteristic length scales selected by the coils. We use cylindrical coordinates defined by $\mathbf{r} = (\rho,\phi,z)$ and locate the 2-D sample in the $z = 0$ plane, the axis of the coil arrangement coinciding with the z axis. Then, in the gauge $\nabla\cdot\mathbf{A} = 0$, Ampère's law for the total vector potential $\mathbf{A}(\mathbf{r})$ can be written as

$$-\nabla^2\mathbf{A}(\rho,z) = \mu_0[\mathbf{K}_s(\rho)\delta(z) + \mathbf{j}_D(\rho,z)], \tag{1}$$

where $\mathbf{j}_D(\rho,z)$ is the current density distribution generated by the drive coil

$$\mathbf{j}_D(\rho,z) = I_D\delta(\rho - R_D)\sum_{n=0}^{N_D-1}\delta(z - h_D - n\delta h_D)\hat{\varphi}. \tag{2}$$

Because of the high degree of precision achieved in controlling the geometrical parameters of the coils in the fabrication process, Eq. (2) is believed to provide a very accurate description of the driving current density. Neglecting normal current contributions and taking an $\exp(i\omega t)$-time dependence for all fields, we define G by $\mathbf{K}_s(\rho) = G(\omega)\mathbf{E}(\rho,z=0) = -i\omega G(\omega)\mathbf{A}(\rho,z=0)$. In writing this local relation, we implicitly assume that finite $\mathbf{q}$ corrections to G can be ignored for the wave vectors selected by our coil configurtion. By Fourier transforming and solving Eq. (1) for $\mathbf{K}_s$ using the formalism developed by Pearl,[8] we obtain

$$\mathbf{K}_s(q_t) = -\frac{\mathbf{j}_D(q_t,q_z = -iq_t)}{1 + (2/i\omega G)q_t}, \tag{3}$$

where q_t and q_z are, respectively, the in-plane and axial components of $\mathbf{q}$. Then, using the driving current distribution of Eq. (2), a straightforward transformation of Eq. (3) back to real space leads to the following expression for $\mathbf{K}_s(\rho)$:

$$\mathbf{K}_s(\rho) = I_D R_D\int_0^\infty dq_t\,\frac{q_t e^{-q_t h_D}}{1 + (2/\mu_0)(1/i\omega G)q_t} \times J_1(q_t R_D)J_1(q_t\rho)\frac{1 - e^{-q_t N_D\delta h_D}}{1 - e^{-q_t\delta h_D}}\hat{\varphi}, \tag{4}$$

where $J_1(x)$ is the first-order Bessel function. As an example, in Fig. 1 we show the screening current distribution resulting from Eq. (4) for the superconducting network described above. At the three temperatures indicated in the figure, this sample behaves as a pure inductor with $G = (i\omega L_k)^{-1}$, where $L_k(T)$ is the network kinetic inductance[6] discussed in detail in the last section of the paper. As expected, $\mathbf{K}_s(\rho)$ has a maximum at $\rho = R_D$, whose strength reflects the linear variation of $L_k^{-1}(T)$ in the temperature range of interest, near the mean-field critical temperature of the network ($T_{c0} = 1.995$ K).

Having found an expression for $\mathbf{K}_s$, we proceed to compute δV by observing that the Fourier transform of the electric field $\delta\mathbf{E}(\rho,z)$ generated by the screening currents flowing in the sample is given by $\delta\mathbf{E}(q_t,q_z) = -i\omega\mu_0\mathbf{K}_s(q_t)/(q_t^2 + q_z^2)$, as follows by inspection of Eq. (1). By performing the line integral of $\delta\mathbf{E}(\rho,z)$ over the N_R equally spaced turns of the lower detection coil (contributions to δV from the upper section of the receiver, being exponentially cut off, can be neglected), we find that δV can be written as

$$\delta V = i\omega I_D\int_0^\infty dx\,\frac{M(x)}{1 + (2/\mu_0 h)(1/i\omega G)x}, \tag{5}$$

where $x = q_t h$, with $h = h_D + h_R$. In this relation, which is the central result of this letter, $M(x)$ is a mutual-inductance distribution comprising the geometry of the measuring system and is given by

$$M(x) = \pi\mu_0 h\alpha\beta J_1(\alpha x)J_1(\beta x)e^{-x}\frac{(1 - e^{-N_D\gamma x})}{(1 - e^{-\gamma x})} \times\frac{(1 - e^{-N_R\delta x})}{(1 - e^{-\delta x})}, \tag{6}$$

where α,β,γ, and δ are, respectively, $R_D, R_R, \delta h_D$, and δh_R expressed in units of h. As illustrated in Fig. 2, for $h = 0.3$ mm, $M(x)$ is strongly peaked at $x\approx 0.2$, a value showing that the relevant Fourier components selected by our coil arrangement have wavelengths of the order of 10 mm. Figure 2 also clearly demonstrates that larger values of h would lead to an appreciable loss of signal.

In the following we describe how the ac conductance of our wire network can be extracted from the response of the sample at 70 kHz, shown as a function of temperature in the upper part of Fig. 3, by applying the numerical inversion procedure of Ref. 4 to Eq. (5). To remove most of the dependence on geometrical parameters, G and δV are conveniently expressed in terms of two complex dimensionless variables, $g \equiv |g|\exp(i\theta_g)$ and $u \equiv |u|\exp(i\theta_u)$, defined by $g = 2/i\omega\mu_0 hG$ and $u = (V_{SS}/\delta V) - 1$, where V_{SS} is the (purely inductive) signal generated by a sample in the strong screening limit ($1/G \to 0$). We determine V_{SS} by measuring the voltage jump at T_{c0} induced by a suitably selected superconducting film showing no observable variations of $\mathrm{Im}[\delta V(T)]$ below T_{c0} ($g \ll 1$) and no detectable evidence of

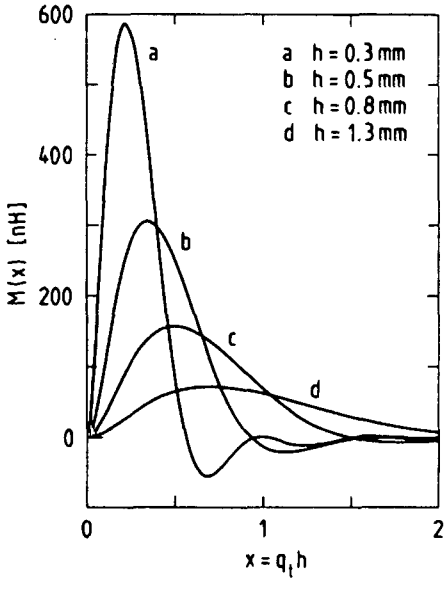

FIG. 2. Geometrical mutual inductance distribution in 2-D q space of the two-coil system shown in Fig. 1 as given by Eq. (6). $h = h_D + h_R$.

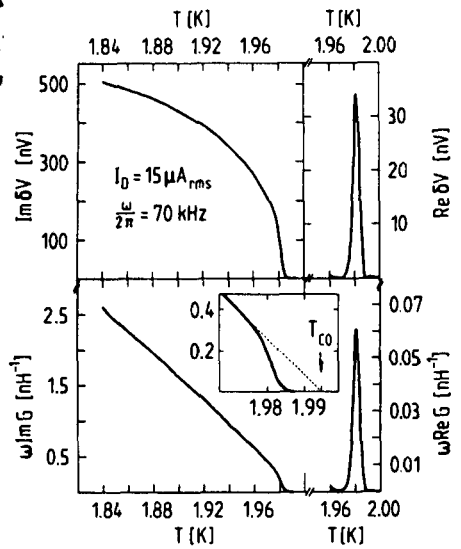

FIG. 3. Upper part: in-phase and quadrature voltage signals vs temperature induced by a superconducting network of Al wires. Lower part: temperature dependence of the complex ac conductance of the network extracted from $\delta V(T)$ by inverting Eq. (5). Inset shows expanded view of the critical region. Dashed straight line is the extrapolated mean field behavior.

eddy currents in the normal state ($g \gg 1$). The measuring system is then calibrated by fitting δ to V_{SS} using Eq. (5). Relying on Eqs. (5) and (6) and on a simple interpolation scheme, two tables, one for θ_u and the other one for the ratio $s = |g|/|u|$, are constructed for a range of values of $|u|$ and θ_g. In both tables, a row corresponds to $|u| = \text{const.}$, while a column is specified by $\theta_g = \text{const.}$ By comparing the data $(|u|,\theta_u)$ with the values in the table for θ_u one reads θ_g and hence, from the corresponding position in the second table, one deduces s, and finally $|g| = s|u|$. Using this simple look-up procedure, we obtain the complex network conductance shown as a function of temperature in the lower part of Fig. 3. With the exception of the critical region, marked by dissipation, the network, as anticipated above, is a pure inductor $[\mathrm{Re}(G) = 0]$ characterized by $\omega\,\mathrm{Im}[G(T)] = L_k^{-1}(T)$. The kinetic inductance is related to the effective penetration depth[6] of the network, $\Lambda(T) = 2(a/w)\lambda^2(T)/d$, where $\lambda(T)$ is the bulk penetration depth, by $L_k(T) = (\mu_0/2)\Lambda(T)$. Thus, as predicted by the Bardeen–Cooper–Schrieffer (BCS) theory[9] at temperatures not too far below T_{c0} one expects $L_k^{-1}(T)$ to be proportional to $(T_{c0} - T)$, in agreement with the observed temperature dependence of $\omega\,\mathrm{Im}[G(T)]$ in Fig. 3. By fitting the inverse kinetic-inductance data of Fig. 3 to the theoretical prediction using the BCS dirty-limit formula for $\lambda(T)$,[9] one finds the value of T_{c0} quoted above and $\lambda(0) = 0.66\ \mu$m [corresponding to $\Lambda(0) = 125\ \mu$m], a value which is within 10% of the theoretical estimate based on the London penetration depth (157 Å), the Pippard coherence length (0.95 μm), and the electronic mean free path (6 Å) of the granular Al film.

In the transition region, the conductance data of Fig. 3 reveal features associated with the critical behavior of the network.[6] At a critical temperature T_c of 1.98 K, just below T_{c0}, we observe a marked drop of the superfluid component accompanied by a peak in dissipation reflecting a phase transition driven by the vortex unbinding mechanism predicted by the Kosterlitz–Thouless theory[10] for 2-D systems. In this connection, it is important to notice that, while there is clear evidence for a "superfluid falloff" at T_c in the imaginary part of the conductance data, almost no trace of this feature is visible in the corresponding signal-voltage data, where it is masked by the convolution of G with the geometry of the coil system described by Eq. (5). This clearly demonstrates the effectiveness of the numerical inversion scheme.

In conclusion, we have shown how a combination of analytical and numerical methods applied to a two-coil mutual-inductance technique provides a powerful tool to study magnetic field penetration effects and critical phenomena in 2-D superconducting systems.

It is a pleasure to thank Ph. Lerch, R. Théron, Ph. Flückiger, R. Rentsch, and R. Meyer for their valuable contributions in developing the two-coil technique and J. R. Clem for providing his unpublished work on screening effects in superconducting films. This work was supported by the Swiss National Science Foundation.

[1] A. T. Fiory and A. F. Hebard, AIP Conf. Proc. **58**, 293 (1980).
[2] A. F. Hebard and A. T. Fiory, Phys. Rev. Lett. **44**, 291 (1980).
[3] A. T. Fiory, A. F. Hebard, and W. I. Glaberson, Phys. Rev. B **28**, 5075 (1983).
[4] A. T. Fiory, A. F. Hebard, P. M. Mankiewich, and R. E. Howard, Appl. Phys. Lett. **52**, 2165 (1988); Phys. Rev. Lett. **61**, 1419 (1988).
[5] Ch. Leemann, Ph. Lerch, G. A. Racine, and P. Martinoli, Phys. Rev. Lett. **56**, 1291 (1986).
[6] B. Jeanneret, Ch. Leemann, and P. Martinoli, Jpn. J. Appl. Phys. **26-3**, 1417 (1987); B. Jeanneret, Ph. Flückiger, Ch. Leemann, and P. Martinoli, IEEE Trans. Magn. **MAG-25**, 1428 (1989); B. Jeanneret, Ph. Flückiger, J. L. Gavilano, Ch. Leemann, and P. Martindi, Phys. Rev. B (to be published).
[7] P. K. Srivastava, P. Debély, H. E. Hintermann, Ch. Leemann, J. Weber, O. Caccivio, P. Martinoli, and H. R. Ott, Physica C **153-155**, 1443 (1988).
[8] J. Pearl, Thesis on: Vortex theory of superconductive memories, Polytechnic Institute of Brooklyn, New York, 1965 (unpublished).
[9] M. Tinkham, *Introduction to Superconductivity* (McGraw-Hill, New York, 1975), p. 80.
[10] M. Kosterlitz and D. J. Thouless, J. Phys. C **6**, 1181 (1973).

DYNAMICAL STUDY OF THE SUPERCONDUCTING PHASE TRANSITION OF TWO-DIMENSIONAL NETWORKS

B. Jeanneret, Ph. Flückiger, Ch. Leemann and P. Martinoli
Institut de Physique, Université de Neuchâtel, 2000 Neuchâtel, Switzerland

Abstract

Granular aluminum wire networks forming square arrays of N x N ≈ 10^6 nodes connected by strips 8 μm long were fabricated with photolithographic techniques. For strip resistances of the order of 1kΩ the superconducting transition of the network, as evidenced by ac conductance measurements, is shown to be of the Kosterlitz-Thouless type. In a perpendicular magnetic field, flux quantization in the loops of the network leads to periodic oscillations of the magnetoconductance.

1. Introduction

Josephson junction arrays and superconducting wire networks[1] provide excellent model systems to study composite materials where superconducting grains or clusters embedded in a non-superconducting matrix are coupled together by the Josephson effect. The situation is comparable to the one encountered in the study of high temperature superconducting ceramics. When compared to granular materials, however, artificial networks offer considerable advantages : their topology, as well as their relevant physical parameters, can be accurately controlled and selected to explore a few specific aspects of an otherwise complex problem.

In this paper we focus our attention on the critical behavior of periodic wire networks. The nature of the superconducting-to-normal transition of wire networks is determined by the ratio a/ξ between the lattice spacing a and the Ginzburg-Landau (GL) coherence length ξ. For $a \ll \xi$ the Josephson coupling energy dominates the condensation energy[2] and, as a consequence, adjacent nodes of the network are strongly coupled to each other. In this case thermal fluctuations in the phase of the complex order parameter at the nodal sites are irrelevant and the phase boundary in the (H,T) plane is obtained by solving a linearized GL equation[3,4]. This strong coupling regime has been extensively investigated by Pannetier and coworkers[5]. The mean field GL approach, however, is no longer valid in the weak coupling limit ($a \gg \xi$), where two-dimensional (2D) phase fluctuations create vortex excitations which are essential in determining the critical behavior of a wire network. According to the Kosterlitz-Thouless (KT) theory[6], applicable to the $a \gg \xi$ case, the transition to the resistive state in zero magnetic field is triggered by the unbinding of vortex pairs and is predicted to occur at a temperature T_c lower than the mean field critical temperature T_{co}. While a vortex unbinding transition has been clearly observed in proximity effect and tunnel junction arrays[1,7,8], for wire networks only limited evidence for KT critical behavior exists[9].

In the following we report a study of the complex ac conductance G of square networks of granular aluminum wires in the critical region. In zero magnetic field the ac response of weakly coupled networks shows, below T_{co}, features which strongly support the existence of a phase transition with KT character. Measurements of the oscillatory ac magnetoconductance of moderately coupled networks are also presented and briefly discussed.

2. Sample Fabrication

Granular aluminum films were evaporated onto silicon wafers held at room temperature. The film thickness d (between 200 Å and 700 Å) and the deposition rate were measured in situ with a standard quartz thickness monitor. The desired resistivity was achieved by carefully adjusting the deposition rate and the partial pressure of oxygen during the evaporation[10]. The samples were then patterned photolithographically, by contact printing a mask produced by electron beam lithography. The final result, shown in Fig. 1, is a network of aluminum wires of width w = 1 μm, forming a square lattice of N x N ≈ 10^6 nodes with lattice parameter a = 8 μm and strip resistance R_s ranging from 10 Ω to 1 kΩ.

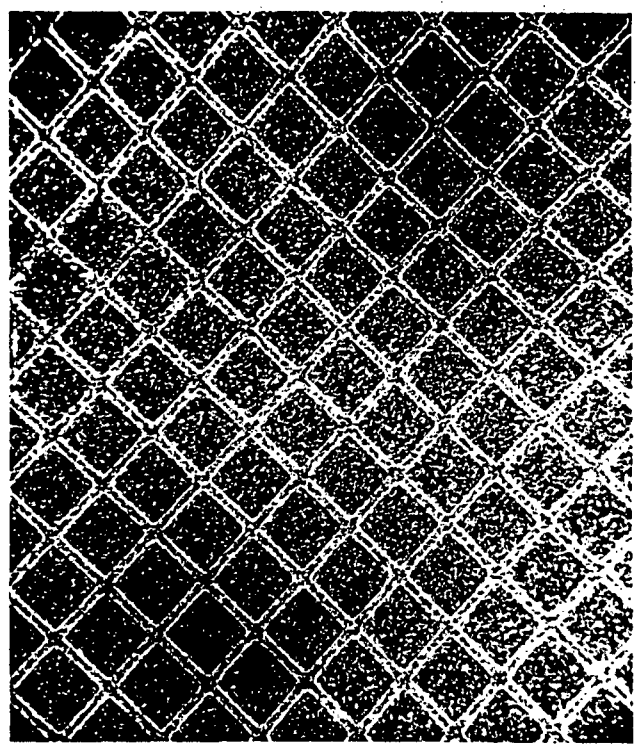

Figure 1. Scanning electron micrograph of an aluminum wire network. The lattice parameter is a = 8 μm.

Since the Josephson coupling energy E_J is proportional to i_c, the critical current of a strip, which in turn is proportional to R_s^{-1} [11], it is possible to cover a wide range of coupling strengths by varying R_s. We found that strip resistances of the order of a few Ohms result in strongly coupled networks with mean field-like behavior. As R_s increases, the nodes slowly decouple, the weak coupling limit being reached when $R_s \sim 1$ kΩ.

Manuscript received August 22, 1988

3. Conductance Measurements

At temperatures below T_{co} the sheet impedance Z of the network is weak. A measuring method which couples directely to the sheet conductance presents therefore a largely increased sensitivity compared to resistive measurements, allowing to test the vortex unbinding mechanism predicted by the KT theory.

The complex conductance $G = Z^{-1}$ of the networks was measured with a mutual inductance detector[1,12] consisting of a cylindrical drive coil and an internal concentric pair of astatic detection coils. A current I_D of angular frequency ω flowing in the excitation coil will induce screening currents in the network which in turn will induce an out-of-balance signal δV in the detection coils. In the weak screening limit[1] this signal is given by

$$\delta V = C\,\omega^2 I_D\, G(\omega,T) \qquad (1)$$

where C is a constant depending of the geometrical parameters of the detector.

At low temperatures, but still in the GL regime, the following mean field behavior is expected :

$$\mathrm{Re}(G) = 0 \qquad (2)$$

$$\mathrm{Im}(G) = \frac{1}{\omega L_k} \qquad (3)$$

where $L_k \propto R_g/(T_{co}-T)$ [9] is the kinetic inductance. In Fig. 2, the real and imaginary parts of the conductance as well as the resistive transition are presented for a weakly coupled network. At low temperatures $\mathrm{Im}(\delta V)$ decreases linearly and $\mathrm{Re}(\delta V) = 0$ as predicted by equation (2) and (3). In the vicinity of the transition however, a dramatic deviation from the mean field prediction occurs. A jump in $\mathrm{Im}(\delta V)$ and a peak in $\mathrm{Re}(\delta V)$ appear in a narrow temperature range below T_{co}. This renormalisation of the conductance is due to vortex excitations predicted by the KT theory, showing that the phase transition is triggered by fluctuations in the phase of the complex order parameter[7].

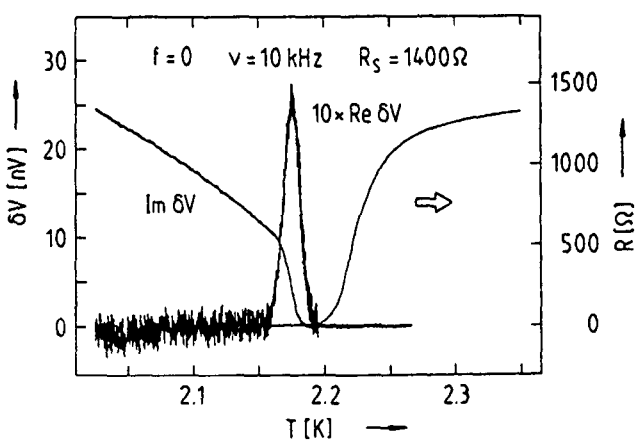

Figure 2. Real and imaginary parts of the conductance of a weakly coupled network, as well as its dc resistance, as a function of temperature.

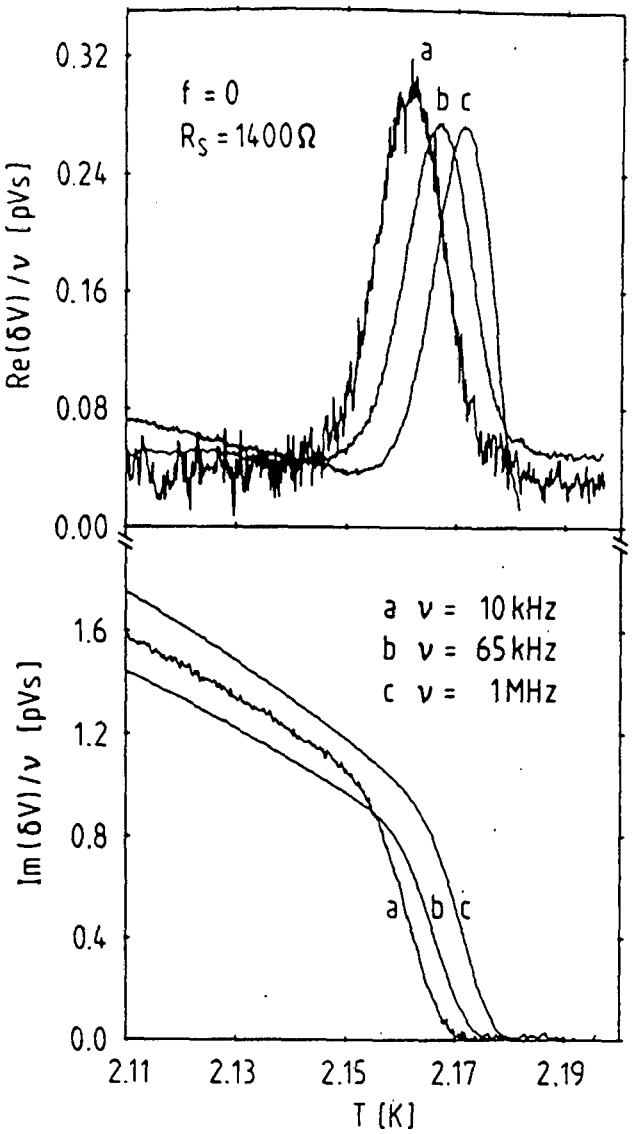

Figure 3. Real and imaginary parts of the ac conductance as a function of temperature at three different frequencies.

With the low temperature linear part of $\mathrm{Im}(\delta V)$ of Fig. 2, we can determine the constant C of equation (1). We find $C = 6.8 \cdot 10^{-17} V^2 s^2/A^2$, in good agreement with the value obtained with a numerical calculation based on the geometrical parameters of the detector. Defining T_c as the temperature corresponding to the break in $\mathrm{Im}(\delta V)$, (T_c = 2.17K), the renormalized value of the kinetic inductance, $L_{kR}(T_c)$, inferred from Fig. 2 and equations (1) and (3), leads to $L_{kR}T_c = 1.32 \cdot 10^{-8}$HK, close to the universal KT prediction $L_{kR}T_c = 1.23 \cdot 10^{-8}$HK [13]. A more detailed analysis of these data will be published elsewhere.

In Fig. 3 experimental curves of the ac response at different frequencies show that the transition temperature is frequency dependent, as expected in a dynamical extension of the KT theory[14]. At the transition temperature T_c vortex-antivortex pairs of infinite size unbind, as the temperature increases beyond T_c, pairs of successively smaller size unbind. At nonzero measuring frequencies only pairs of size smaller than the probing length r_ω contribute to the response[14]. Since r_ω decreases with frequen-

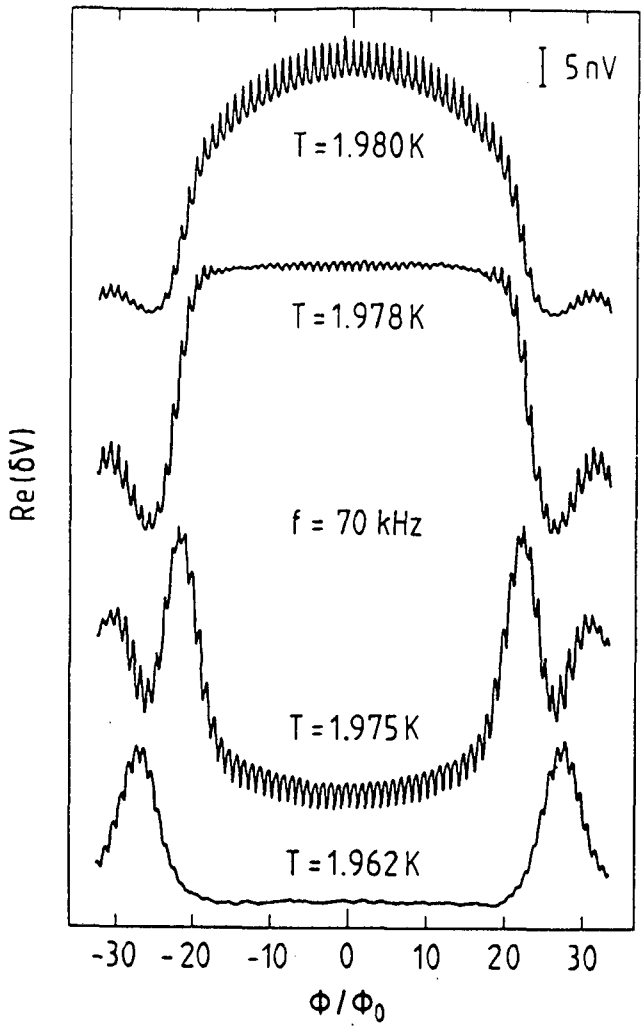

Figure 4a. Real part of the magnetoconductance for a sample with $R_S \simeq 10^2\Omega$ at four different temperatures.

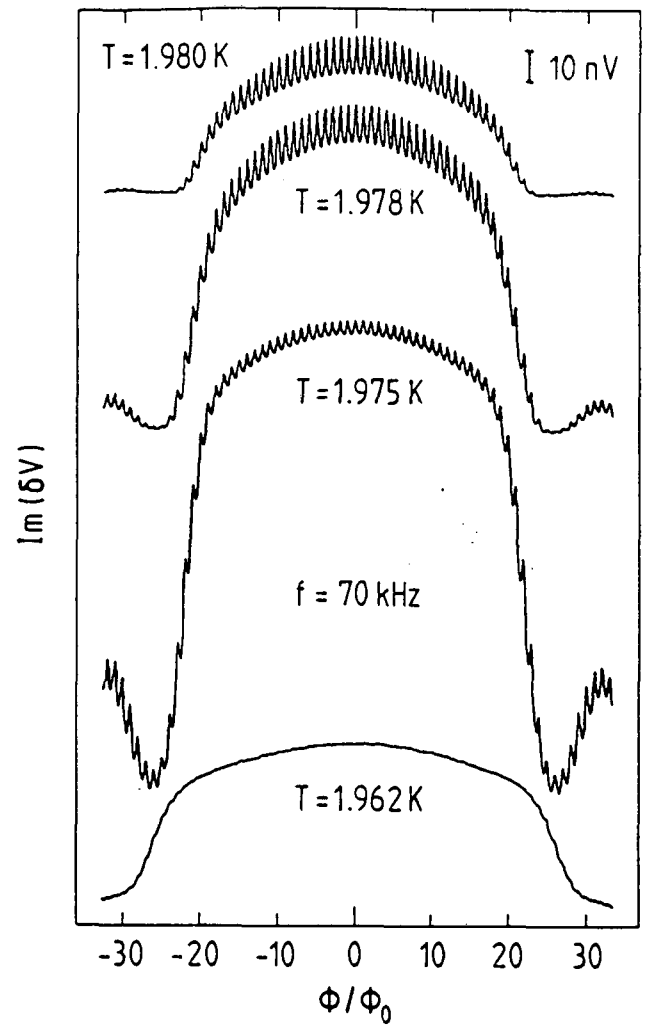

Figure 4b. Imaginary part of the magnetoconductance for a sample with $R_S \simeq 10^2\Omega$ at four different temperatures.

cy, the transition temperature is observed at higher temperatures as the frequency is increased, in accordance with the measurements reported in Fig. 3.

4. Magnetic Field Effects

In a perpendicular magnetic field a regular network in the transition region is uniformly frustrated with a frustration parameter f given by the applied magnetic flux per unit cell in units of the superconducting flux quantum[1]. The real and imaginary parts of the ac conductance as a function of f at four different temperatures is shown in Fig. 4, for a sample with $R_S \simeq 10^2\ \Omega$. In a small temperature range below T_{co} both components of δV show oscillations of period unity persisting out to $f \sim 40$, indicating a high degree of sample uniformity. In lower resistance samples structures at small half integer f-values have also been observed[9]. The complexity of the envelope of the signals of Fig. 4 is at present not well understood in every detail. Its main features, however, can be qualitatively understood by taking into account two effects : the reduction of the mean field transition temperature due to the magnetic field, and a diffraction-like modulation due to the dependence of i_c on B in a single strip.

As an example of the effect of the magnetic field onto T_{co}, consider the $T = 1.975$ K curve of Fig. 4a: at low magnetic fields, flux quantization in the unit cells dominates and the signal returns to its $f = 0$ value every $\Delta f = \pm 1$. Gradually, however, the magnetic field lowers T_{co}; as a result, while at $f = 0$ we were to the left of the peak of Fig. 2, at $f \sim 20$ the signal has reached its peak value, and then slowly decreases again.

The diffraction-like pattern is most easily observed in the $T = 1.975$ K curve of Fig. 4b where the minimum at $f = 27$ is believed to correspond to one flux quantum in each strip. This interpretation is supported by two observations : the applied magnetic field corresponds to one flux quantum in an area of the order of $\omega\xi(T)$ and the minimum shifts to higher field values as the temperature is lowered, in accordance with the temperature dependence of $\xi(T)$.

5. Conclusions

The unique features of the dynamics of vortex excitations can be most sensitively probed with an experimental method measuring directly the sheet conductance of the samples.

The properties of regular wire networks, as investigated with ac conductance measurements, show that the KT transition can indeed be observed in weakly coupled samples. The temperature dependence and, albeit only qualitatively, the frequency dependence of their ac response presented here are in agreement with a description of the critical behavior in terms of the KT vortex unbinding mechanism.

Dr. J. Beguin's scanning electron micrograph, useful discussions with Dr. J.L. Gavilano and technical assistance by U. Mohr are gratefully acknowledged. This work was supported by the Fonds National Suisse pour la Recherche Scientifique.

References

[1] P. Martinoli, Ph. Lerch, Ch. Leemann, and H. Beck, "Arrays of Josephson Junctions.: Model systems for Two-Dimensional Physics", Jpn. J. Appl. Phys., vol. 26-3, p. 1999, 1987.

[2] J. R. Clem, "Granular and superconducting-glass properties of the high-temperature superconductors", Physica C, vol. 153-155, p. 50, 1988.

[3] S. Alexander and E. Halevi, "Superconductivity on networks : II. The London approach", J. Physique, vol. 44, p. 805, 1983.

[4] S. Teitel and C. Jayaprakash, "Resistive transitions in regular superconducting wire networks", J. Physique Lett., vol. 46, p. L33, 1985.

[5] B. Pannetier, J. Chaussy and R. Rammal, "Experimental Fine Tuning of Frustration : Two-Dimensional Superconducting Network in a Magnetic Field", Phys. Rev. Lett., vol. 53, p. 1845, 1984.

[6] J. M. Kosterlitz and D. J. Thouless, "Ordering, metastability and phase transitions in two-dimensional systems", J. Phys. C, vol. 6, p. 1181, 1973.

[7] Ch. Leemann, Ph. Lerch, G.-A. Racine and P. Martinoli, "Vortex Dynamics and Phase Transitions in a Two-Dimensional Array of Josephson Junctions", Phys. Rev. Lett., vol. 56, p. 1291, 1986.

[8] B. J. van Wees, H. S. van der Zant and J.E. Mooij, "Phase transitions of Josephson-tunnel-junction arrays at zero and full frustration", Phys. Rev. B, vol. 35, p. 7291, 1987.

[9] B. Jeanneret, Ch. Leemann and P. Martinoli, "Dynamics of the Phase Transition of Periodic Superconducting Networks", Jpn. J. Appl. Phys., vol. 26-3, p. 1417, 1987.

[10] G. Deutscher, H. Fenichel, M. Gershenson, E. Grünbaum and Z. Ovadyahu,"Transition to Zero Dimensionality in Granular Aluminum Superconducting Films", J. Low. Temp. Phys., vol. 10, p. 231, 1973.

[11] V. Ambegaokar and A. Baratoff, "Tunneling between superconductors", Phys. Rev. Lett., vol. 10, p. 486, 1963.

[12] A. F. Hebard and A. T. Fiory, "Evidence for the Kosterlitz-Thouless Transition in Thin Superconducting Aluminum Films", Phys. Rev. Lett., vol. 44, p. 291, 1980.

[13] C. J. Lobb, D. W. Abraham and M. Tinkham, "Theoretical interpretation of the resistive transition data from arrays of superconducting weak links", Phys. Rev. B, vol. 27, p. 150, 1983.

[14] V. Ambegaokar, B. I. Halperin, D. R. Nelson, and E. D. Siggia, "Dissipation in Two-Dimensional Superfluids", Phys. Rev. Lett., vol. 40, p. 783, 1978.

PHYSICAL REVIEW B VOLUME 40, NUMBER 16 1 DECEMBER 1989

Critical phase fluctuations in superconducting wire networks

B. Jeanneret, Ph. Flückiger, J. L. Gavilano, Ch. Leemann, and P. Martinoli
Institut de Physique, Université de Neuchâtel, 2000 Neuchâtel, Switzerland
(Received 21 September 1989)

A study of the onset of superconducting phase coherence in periodic wire networks with weakly coupled adjacent nodes is presented. In a narrow temperature range below the mean-field critical temperature, ac conductance measurements reveal a drop in superfluid density and a peak in dissipation providing the first observation in networks of the vortex unbinding transition predicted by the Kosterlitz-Thouless theory. The ac response in the critical region is accurately described by dynamical extensions of the theory incorporating vortex-pinning phenomena created by the periodic structure of the network.

Networks of superconducting wires and arrays of Josephson weak links[1] prepared by modern lithographic techniques provide excellent systems to study fundamental concepts of condensed matter and statistical physics. Particularly attractive is the possibility of using these systems as testing grounds for the theoretical ideas of scaling, renormalization, frustration, and randomness underlying the physics of critical phenomena in two dimensions.

In this paper we explore the nature of the superconducting-to-normal (SN) transition (in zero magnetic field) of periodic two-dimensional (2D) wire networks[2] in the limiting case of weakly coupled nearest-neighbor nodes. Relying on a two-coil mutual-inductance method[3] to study the ac superfluid response of the system to a small oscillating driving field, we observe features in the critical region which provide strong evidence for a phase transition triggered by the vortex unbinding mechanism of the Kosterlitz-Thouless (KT) theory.[4] This conclusion is corroborated by a detailed study of the response based on dynamical extensions[5] of the KT theory. An important and distinctive aspect of our experiments, the fluctuating Brownian motion of vortex excitations in the periodic pinning potential created by the network, was included in the theoretical treatment and is shown to have a profound effect on the characteristic length scales probed in the ac measurements. The quality of the fit between theory and experiment emerging from our analysis is remarkable, comparable to that found so far only in studies of the superfluid transition in liquid-helium films[6] and in indium oxide films.[7] The results presented here are the first to show the KT transition in a network of superconducting wires. Previous work[2] on this system was performed in the strong-coupling regime, where the phase boundary in the (H,T) plane was found to be accurately described by the mean-field Ginzburg-Landau (GL) theory.

The nature of the SN transition of wire networks depends on the ratio a/ξ between the network lattice spacing a and the GL coherence length $\xi(T)$. Inspection of the GL free energy of the system[8] shows that for $a \ll \xi$ Josephson coupling between adjacent nodes is strong, the coupling energy being a factor $(2\xi/a)^2$ larger than the condensation energy in the interconnecting link. In this limit fluctuations in the phase ϕ_i of the complex order parameter at the nodal sites are irrelevant and the SN phase boundary of the network in the (H,T) plane is obtained by solving a linearized GL equation.[2]

The critical behavior of weakly coupled $(a \gg \xi)$ wire networks is radically different from that predicted by the mean-field GL approach. In this regime, below the mean-field critical temperature T_{co}, 2D phase fluctuations are essential to determine the nature of the SN transition, while amplitude fluctuations can be ignored. Assuming a position-independent order-parameter amplitude, which appears to be justified for $a \gg \xi$, the coupling energy of nearest-neighbor nodes takes on the piecewise parabolic dependence on $(\phi_i - \phi_j)$ characteristic of long $(a \gg \xi)$ microstrips with a piecewise linear current-phase relation.[9] The resulting expression of the free energy[8] shows that weakly coupled wire networks belong to the class of classical XY models with a temperature-dependent coupling energy given by[9]

$$E_J(T) = (\pi/4)(R_u/R_s)\Delta(T)\tanh[\Delta(T)/2k_BT],$$

where $\Delta(T)$ is the BCS gap parameter, R_s the normal-state strip resistance, and $R_u = \hbar/e^2$. According to the KT theory, the (zero field) critical behavior of the system is governed by 2D-phase fluctuations in the form of quantized vortices, the transition to the resistive state being driven by the unbinding of vortex-antivortex pairs at a critical temperature T_c lower than T_{co}.[9]

To ascertain this prediction, square wire networks with $a = 8$ μm containing about 10^6 nodes were photolithographically patterned from 200-Å-thick granular aluminum films. An appreciable reduction of T_c below T_{co} ($T_{co} - T_c \approx 100$ mK) and an $a/\xi(T_c)$ ratio of the order of 100 were obtained by an appropriate choice of the strip width ($w \approx 0.8$ μm) and of the normal-state resistivity of the Al films ($\rho \approx 150$ $\mu\Omega$ cm). The onset of 2D superconducting phase coherence in the networks was probed by studying their ac screening properties with an inductive technique.[3] The method consists of exposing the network to a weak ac magnetic field created by a 4-mm-diam drive coil located just above the sample. The excitation level, chosen to ensure a linear response, reached a maximum rms value of ~ 0.4 mG at the center of the network, while ambient magnetic fields were suppressed to ~ 1 mG. The response of the sample to the ac field was measured by

detecting the in-phase and quadrature components of the signal δV induced by the screening currents in a pair of astatic 2-mm-diam coils coaxially mounted within the drive coil. Data were taken at angular frequencies ω ranging from $\sim 6\times10^3\ s^{-1}$ to $\sim 6\times10^7\ s^{-1}$.

Figure 1 shows, emphasizing the critical-temperature region, the complex ac response $\delta V(T)$ measured at 10, 65, and 1000 kHz of an Al network with $R_s = 750\ \Omega$. Since the weak screening condition is almost satisfied at the temperatures of interest, $\delta V(T)$ is, to a first approximation, proportional to the complex ac conductance $G(T)$ of the sample.[3] In particular, $\mathrm{Im}[\delta V(T)]$ reflects the temperature dependence of the inverse kinetic inductance $L_K^{-1}(T)$ which measures the effective (renormalized) areal superfluid density in the network.[9] As shown in Fig. 1, in a narrow temperature range ($\Delta T \approx 30$ mK) centered about a frequency-dependent critical temperature T_ω we observe a marked drop in superfluid density, while a peak, whose position is used to locate T_ω, grows in the dissipative part $\mathrm{Re}[\delta V(T)]$ of the signal. These features are quite similar to those observed in ac measurements of the superfluid transition of other 2D systems[6,7,10,11] and as discussed in detail below, can be accurately described by dynamical theories[5] based on the KT vortex unbinding idea.

Also shown in Fig. 1 (upper part) is the dc resistive transition of the network. On the high-temperature side above T_{co}, fluctuations in the order-parameter amplitude lower the network sheet resistance below its normal-state value R_s. To obtain an estimate of T_{co}, the inverse excess conductance $(R^{-1}-R_s^{-1})^{-1}$ was fitted to the Aslamasov-Larkin theory[12] for fluctuation-induced superconductivity in two dimensions using T_{co}, R_s, and R_u as adjustable parameters.[7] From the fit, shown in the lower part of Fig. 1, we deduce $T_{co} = 2.236$ K, $R_s = 750\ \Omega$, and $R_u = 4.94$ kΩ (the theoretical value of R_u is 4.11 kΩ). The uncertainty in the determination of T_{co} is 25 mK.

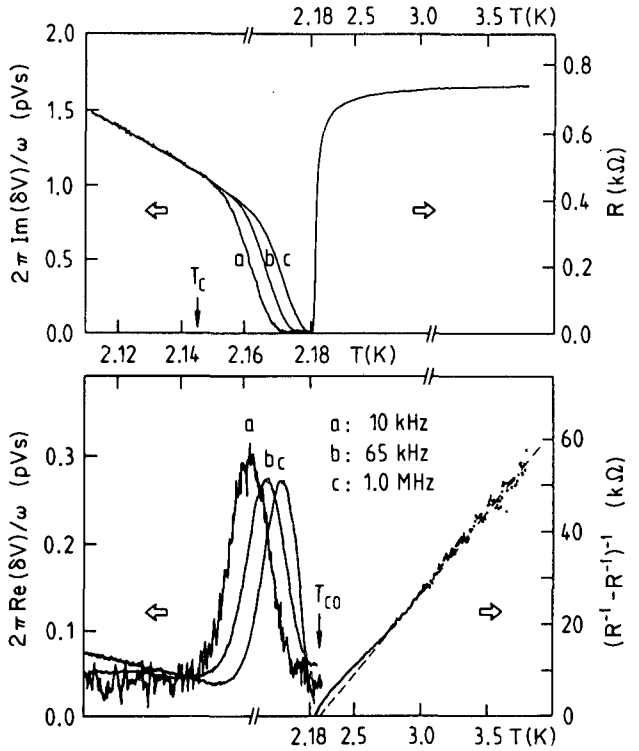

FIG. 1. Complex ac response vs temperature of a weakly coupled wire network measured at different frequencies near the superconducting transition. Also shown are the resistive transition (upper part) and the inverse excess conductance above T_{co} (lower part). The dashed line is a fit to the Aslamasov-Larkin theory.

The quantity to be compared with theory is the complex ac conductance rather than the signal voltage. Accordingly, G was calculated from the δV data by numerically solving the integral equation relating δV to G for our specific sample-coil configuration.[3] An example is shown in Fig. 2, where real and imaginary parts of ωG, as deduced from the 65-kHz response of Fig. 1, are plotted as a function of temperature and compared with the following prediction of the dynamical theory:[5,9]

$$G^{-1}(T,\omega) = [\omega L_{K0}(T)/\tilde{T}][\pi^4 y^2(l_\omega,\tilde{T}) + iK^{-1}(l_\omega,\tilde{T})] + R(\tilde{T})[a/\xi_+(\tilde{T})]^2, \quad (1)$$

where $L_{K0}(T) = (\hbar/2e)^2/E_J(T)$ is the kinetic inductance in the absence of thermal fluctuations. Equation (1) shows the decomposition of the network impedance G^{-1} in contributions from bound vortex pairs and from free vortices. The complex vortex-pair contribution is expressed in terms of two scale-dependent $[l \equiv \ln(r/a)]$ and temperature-dependent $[\tilde{T} \equiv k_B T/E_J(T)]$ quantities: the reduced stiffness K and the vortex excitation probability y. The characteristic length scale probed in the ac measurements is the vortex diffusion length $r_\omega \approx (14\mu k_B T/\omega)^{1/2}$, where μ is the vortex mobility discussed below in connection with thermally activated vortex motion in the periodic potential provided by the network. The renormalization procedure based on the Kosterlitz recursion equations[9,13] allows K and y to be computed for $l = l_\omega$ once their initial values at $l = 0$ are known. Adopting Mooij's notion,[9] we take $K(0,\tilde{T}) = \tilde{T}^{-1}$ and $y(0,\tilde{T}) = N_0 \exp(-2\pi\gamma/\tilde{T})$,

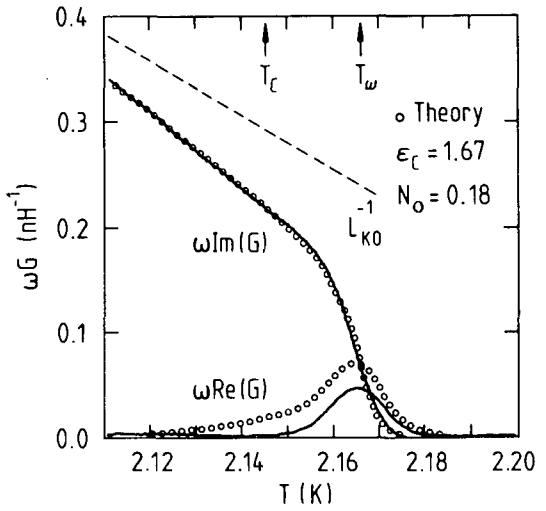

FIG. 2. Experimental (solid curves) and theoretical (open circles, see text) complex ac conductance at 65 kHz of the network of Fig. 1 as a function of temperature near the superconducting transition. The dashed line is the GL mean-field prediction.

where N_0 and γ are nonuniversal parameters related to the vortex-core energy. Above T_c, the theoretical prescription $y(l_+,\tilde{T})=y(0,\tilde{T})$ for truncating the renormalization process introduces a new length scale, the correlation length $\xi_+(\tilde{T})\equiv ae^{l_+(\tilde{T})}$ which measures the average distance between free vortices.

Unlike vortex excitations in ideal superconducting films, vortices in networks experience the pinning effect due to the underlying periodic structure. Using a continued-fraction method, it is possible to estimate the ac vortex mobility in networks by studying the Brownian motion of an individual vortex exposed, for simplicity, to a sinusoidal force field.[14] At the low frequencies used in our experiments, the result is

$$\mu(T)=(a/\phi_0)^2R(T)=(a/\phi_0)^2R_s[I_0(U/2k_BT)]^{-2};$$

where $I_0(x)$ is the modified Bessel function of order zero and U the potential barrier created by the interconnecting links. To estimate the activation energy, we observe that in the critical region the strip width is such that $w/\xi\gg 1$ [typically, $w/\xi(T_\omega)\approx 10$], thereby requiring the nucleation of a normal vortex core during the link crossing process.[15] Thus, U will be almost entirely determined by the condensation energy associated with the core nucleation process. Using Clem's vortex model,[16] we find $U/2k_BT\approx(\pi a/4w)\tilde{T}^{-1}$. In our networks the a/w ratio is so large ($a/w\approx 10$) that, because of the exponential character of $I_0(x)$ for $x\gg 1$, $\mu(T)$ drops by several orders of magnitude in a narrow temperature range below T_{co}, thereby causing the drastic reduction of l_ω which accounts for the observed broadening of the transition. At sufficiently low temperatures, however, vortex pinning and vortex-vortex correlations become so strong that a model based on the Brownian motion of a single vortex excitation is no longer appropriate and the theory is expected to fail. A manifestation of this failure is the "reentrant" behavior of Re[$G(T)$] (not shown in Fig. 2) predicted by the model below a certain temperature $T^*<T_\omega$ ($T^*\approx 2.15$ K in Fig. 2). The origin of this unphysical feature can be traced back to the very short length scales entering renormalization for $T<T^*$. This suggests interpreting the characteristic length at T^*, $r_\omega(T^*)$, as the shortest length scale consistent with the model. Accordingly, in the calculations presented below, $l_\omega(T)$ was kept fixed at $l_\omega(T^*)$ for $T<T^*$ [$l_\omega(T^*)\approx 0.8$ in Fig. 2].

Setting $U/2k_BT\approx a\tilde{T}^{-1}$, the ac conductance data of Fig. 2 were fitted to Eq. (1) using N_0, a, γ, and T_{co} as adjustable parameters (R_s was kept at 750 Ω). An excellent fit of the inductive component is obtained for $N_0=0.18$, $2\pi\gamma=0.82$, $a=7.85$, and $T_{co}=2.258$ K, while the computed dissipative component sets in at temperatures too low to agree with the data. However, considering the high sensitivity of the response to vortex pinning and the approximate method used to incorporate its effect in the dynamical theory, we feel that dissipation is, on the whole, remarkably well described by our model. The value of a is in very good agreement with the predition of Clem's model, whereas T_{co} is consistent with the result extracted from the paraconductivity contribution to the dc conductance above T_{co}. Using a and T_{co} as deduced from the fit, we can estimate the typical length scales explored at 65 kHz: we find $l_\omega=1.13$ ($r_\omega=3.1a$) at $T_\omega=2.166$ K. From the expression relating N_0 and γ to the vortex dielectric constant ϵ_c (Ref. 9) we find $\epsilon_c=1.67$, a value in good agreement with the result ($\epsilon_c\approx 1.70$) of Monte Carlo simulations.[17] Finally, from the universal prediction $K^{-1}(\infty,\tilde{T}_c)=\epsilon_c\tilde{T}_c=\pi/2$ we obtain $T_c=2.146$ K.

As demonstrated by the data of Fig. 1 and predicted by the dynamical theory, the vortex unbinding transition shifts to higher temperatures with increasing ω. If one identifies T_ω as the temperature where the crossover from a vortex-pair- to a free-vortex-dominated response occurs, then T_ω is implicitly defined by $r_\omega(\tilde{T}_\omega)\approx\xi_+(\tilde{T}_\omega)$.[5] To test this fundamental prediction, $r_\omega(\tilde{T}_\omega)$ was deduced from the measured T_ω, while $\xi_+(\tilde{T})$ was computed from the theoretical prescription $y(l_+,\tilde{T})=y(0,\tilde{T})$. All calculations were consistently performed with the parameter values which fit the data of Fig. 2. The results, expressed in terms of the dimensionless quantities l_ω^{-2} and l_+^{-2}, are shown in Fig. 3 as a function of the reduced-temperature shift $(\tilde{T}_\omega-\tilde{T}_c)$. For small shifts (low ω) the scaling parameter inferred from experiment (l_ω) is in excellent agreement with theory (l_+), whereas deviations from the predicted behavior occur for large shifts of T_ω (high ω). This might be due to the fact that the KT theory is less accurate at temperatures well above T_c. Figure 3 also shows that the large length scales required to explore the region very close to T_c were not accessible in our experiments. In this temperature range $l_+^{-2}(\tilde{T})$ is predicted[4,13] to assume the asymptotic form $l_+^{-2}=b(\tilde{T}-\tilde{T}_c)$. If b is consistently computed[9] from N_0 and ϵ_c ($b=0.51$), the data cannot be fitted by this expression, which is obeyed only in a very narrow (~2 mK) interval just above T_c. In light of this result, evidence for the square-root singularity of $l_+(\tilde{T})$ found in previous work[9,10] should be reconsidered.

In conclusion, measurements of the complex ac conductance of weakly coupled superconducting wire networks

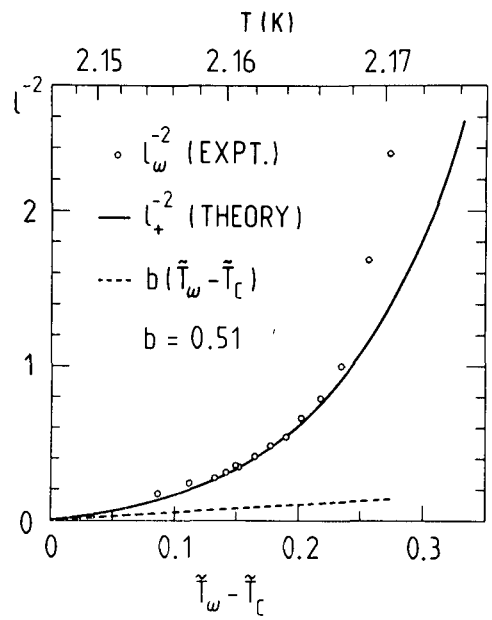

FIG. 3. Dependence of the scaling parameter l_ω on the shift of the dimensionless vortex-unbinding temperature $\tilde{T}_\omega$. The solid line is the prediction of the dynamical KT theory, the dashed line its asymptotic form very close to T_c.

have provided the first observation of the Kosterlitz-Thouless vortex unbinding transition in this system. The remarkable degree of quantitative agreement emerging from the theoretical analysis of the dynamic response suggests that weakly coupled wire networks will also be ideal model systems for studies of critical phenomena in frustrated and/or disordered two-dimensional systems. Apart from their intrinsic fundamental importance, such investigations should provide a deeper understanding of some of the intriguing magnetic properties of high-temperature superconducting ceramics.

We would like to thank H. Beck for many stimulating discussions and U. Mohr, D. Varidel, and Y. Oppliger for technical assistance. This work was supported by the Swiss National Science Foundation.

[1]For a recent review of the field, see *Coherence in Superconducting Networks,* edited by J. M. Mooij and G. B. J. Schön [Physica B **152**, Nos. 1 and 2 (1988)].

[2]B. Pannetier, J. Chaussy, R. Rammal, and J. C. Villegier, Phys. Rev. Lett. **53**, 1845 (1984).

[3]A. T. Fiory and A. F. Hebard, in *Inhomogeneous Superconductors—1979,* edited by D. U. Gubser, T. L. Francavilla, S. A. Wolf, and J. R. Leibowitz, AIP Conf. Proc. No. 58 (American Institute of Physics, New York, 1979), p. 293; A. T. Fiory, A. F. Hebard, P. M. Mankiewich, and R. E. Howard, Appl. Phys. Lett. **52**, 2165 (1988); B. Jeanneret, J. L. Gavilano, G. A. Racine, Ch. Leemann, and P. Martinoli, Appl. Phys. Lett. (to be published).

[4]J. M. Kosterlitz and D. J. Thouless, J. Phys. C **6**, 1181 (1973).

[5]V. Ambegaokar, B. I. Halperin, D. R. Nelson, and E. D. Siggia, Phys. Rev. B **21**, 1806 (1980); S. R. Shenoy, J. Phys. C **18**, 5163 (1985).

[6]D. J. Bishop and J. D. Reppy, Phys. Rev. B **22**, 5171 (1980).

[7]A. T. Fiory, A. F. Hebard, and W. I. Glaberson, Phys. Rev. B **28**, 5075 (1983).

[8]S. Teitel and C. Jayaprakash, J. Phys. (Paris) Lett. **46**, L33 (1985).

[9]J. E. Mooij, in *Percolation, Localization and Superconductivity,* edited by A. M. Goldman and S. A. Wolf (Plenum, New York, 1984), p. 325.

[10]Ch. Leemann, Ph. Lerch, G.-A. Racine, and P. Martinoli, Phys. Rev. Lett. **56**, 1291 (1986).

[11]A. T. Fiory, A. F. Hebard, P. M. Mankiewich, and R. E. Howard, Phys. Rev. Lett. **61**, 1419 (1988).

[12]L. G. Aslamasov and A. I. Larkin, Fiz. Tverd. Tela. **10**, 1104 (1968) [Sov. Phys. Solid State **10**, 875 (1968)].

[13]J. M. Kosterlitz, J. Phys. C **7**, 1046 (1974).

[14]P. Martinoli, M. Nsabimana, G.-A. Racine, H. Beck, and J. R. Clem, Helv. Phys. Acta **56**, 765 (1983).

[15]K. K. Likharev, Rev. Mod. Phys. **51**, 101 (1979).

[16]J. R. Clem, J. Low Temp. Phys. **18**, 427 (1975).

[17]S. Teitel and C. Jayaprakash, Phys. Rev. B **27**, 598 (1983).